Industrial Crops & Products 222 (2024) 119850

Contents lists available at ScienceDirect

Industrial Crops & Products

journal homepage: www.elsevier.com/locate/indcrop

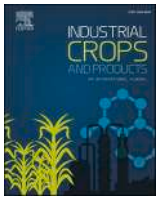

HaVTE1 confers ABA insensitivity by blocking the ABA signaling pathway in sunflowers (*Helianthus annuus* L.)

Yingwei Wang [a], Jiafeng Gu [a], Qinzong Zeng [a], Xinxin Li [a], Yuliang Han [a], Qinyu Xie [a], Chenchang Wang [a], Zhonghua Lei [b], Qixiu Huang [b], Lijun Xiang [b], Juncheng Zhang [a], Hada Wuriyanghan [c], Maohong Cai [a,*], Tao Chen [a,*]

[a] *Zhejiang Provincial Key Laboratory for Genetic Improvement and Quality Control of Medicinal Plants, College of Life and Environmental Science, Hangzhou Normal University, Hangzhou 311121, China*
[b] *Institute of Economic Crops, Xinjiang Academy of Agricultural Sciences, Urumqi 830000, China*
[c] *Key Laboratory of Forage and Endemic Crop Biotechnology, Ministry of Education, School of Life Sciences, Inner Mongolia University, Hohhot 010070, China*

ARTICLE INFO

Keywords:
VTE1
Tocopherol cyclase
ABA signaling pathway
Sunflower
Abiotic stress

ABSTRACT

Sunflower (*Helianthus annuus*) is the fourth major oilseed crop in the world, with remarkable tolerance in saline-alkali soils. The *VTE1* gene encodes tocopherol cyclase (TC), an enzyme pivotal in the biosynthesis of both vitamin E and vitamin K1. Despite its integral role in the synthesis of these crucial vitamins, the functional analysis of *VTE1* under abiotic stress in sunflowers remains scant. In the present investigation, a structural analysis of the VTE1 protein across 155 diverse species revealed a highly conserved evolutionary trace. The expression profiling of *HaVTE1* depicted that the *HaVTE1* was responsive to the ABA pathway. Transgenic results confirmed that overexpression of *HaVTE1* in *Arabidopsis* and sunflower showed decreased sensitivity to ABA while knocking-down in sunflower exhibited the opposite phenotype. Furthermore, biochemical experiments displayed that *HaVTE1* decreases ABA sensitivity by scavenging superoxide contents. Concurrently, the transcriptome analysis revealed that *HaVTE1* blocked the upstream of the ABA signaling cascade, which was further confirmed by luciferase assay, resulting in reduced sensitivity to ABA of *HaVTE1* overexpression plants. The findings shed light on a theoretical basis for the sunflower responses to ABA signaling and abiotic stresses.

1. Introduction

Sunflower (*Helianthus annuus* L.), a member of the Asteraceae family, is characterized by its remarkable resistance to saline-alkali stress, drought, and nutrient deficiency conditions, as well as its robust adaptability. These attributes have enabled sunflower extensive cultivation, particularly in America, Europe, and the north of Asia. Consequently, elucidating the molecular mechanism of sunflower's resistance to abiotic stresses offers not only a theoretical basis for targeted breeding but also innovative strategies for optimizing stress tolerance in other plant species. Previously, HaWRKY76 has been reported to confer tolerance to both dehydration and submergence in Arabidopsis transgenic lines, remarkably without any yield penalty (Raineri et al., 2015). Overexpressing of sunflower TLDc-containing protein Oxidation Resistance 2 (*HaOXR2*) in Arabidopsis and maize increases the blade area of plant as well as the oxidative stress tolerance, implying a conserved functional role of *HaOXR2* across dicot and monocot species (Torti et al., 2020). Furthermore, HaHB11, a multifaceted homeodomain-leucine zipper (HD-Zip) transcription factor, has been shown to enhance the yield and biomass of transgenic plants, as well as augment the flooding tolerance (Cabello et al., 2016). Additionally, HaHB11 confers drought and salinity tolerance via a sophisticated mechanism encompassing morphological, physiological and molecular processes, which include the induction of leaf rolling and root elongation (Cabello et al., 2017). HaHB-4, another HD-Zip transcription factor, serves as the junction between the drought response and the ethylene signaling pathway (Dezar et al., 2005; Manavella et al., 2006). In addition, comprehensive omics analysis and genome-wide association studies have been employed to excavate potential resistance genes in sunflowers (Ceylan et al., 2023; Moschen et al., 2017; Ramu et al., 2016; Song et al., 2022).

Vitamin E biosynthesis requires a set of enzymes, such as HPPD and VTE1–4, whose overexpression can increase VTE content in plants

* Corresponding authors.
E-mail addresses: caimaohong@hznu.edu.cn (M. Cai), chentao@hznu.edu.cn (T. Chen).

https://doi.org/10.1016/j.indcrop.2024.119850
Received 23 May 2024; Received in revised form 8 October 2024; Accepted 10 October 2024
Available online 19 October 2024

(Kanwischer et al., 2005; Lee et al., 2007). Among these genes, *HPPD* and *VTE1* have been reported to be associated with stress resistance (Ellouzi et al., 2013; Havaux et al., 2005; Kim et al., 2021; Kobayashi and DellaPenna, 2008; Liu et al., 2008; Rastogi et al., 2014). We found that abundant studies have shown that VTE1 can enhance plant stress, especially in plant abiotic stress, which is the most reported. *VTE1* gene encodes the enzyme tocopherol cyclase (TC), which plays a dual role in the biosynthesis of essential lipophilic antioxidants. It not only transforms 2-methyl-6-phytyl-1,4-benzoquinol (MPBQ) or 2,3-dimethyl-5--phytyl-1,4-benzoquinone (DMPBQ) into δ- or γ- tocopherol but also converts phylloquinone hydroquinone (PQH2–9) into phytylmenaquinone (PC8) in the production of vitamin K1 (Spicher and Kessler, 2015). Previous studies focused on the physiological and biochemical properties and antioxidant function of *VTE1*. Notably, VTE1 holds the distinction of being the first gene unearthed within the vitamin E synthesis pathway. Its discovery was facilitated by screening of maize mutants that exhibited the phenotype of accumulation of anthocyanins and starch within leaf blades (Provencher et al., 2001). Despite *Solanum tuberosum StSXD1*-silenced transgenic plants showing a defect in photoassimilate export similar to the maize *sxd1* mutant, Arabidopsis orthologous mutant *vte1* lacks this phenotype, suggesting a divergence in tocopherol function between C4 and C3 plants (Hofius et al., 2004). Meanwhile, *vte1* is devoid of tocopherol while the overexpression of *VTE1* increases the total tocopherol content in leaves, and a dramatic shift from α-tocopherol to γ-tocopherol (Kanwischer et al., 2005). Additionally, the *vte1* phenotype exhibits accelerated senescence (Simancas and Munné-Bosch, 2015) and reduces seed longevity (Sattler et al., 2004). Moreover, *VTE1* confers plant-enhanced tolerance to both abiotic and biotic stress (Ma et al., 2020). Illustratively, overexpressing *AtVTE1* in tobacco enhances tolerance to drought stress (Liu et al., 2008). In *Oryza sativa*, abiotic stresses such as NaCl, H_2O_2, and ABA significantly induce *OsVTE1* expression, with *OsVTE1* overexpression lines demonstrating heightened salt stress tolerance (Ouyang et al., 2011). Arabidopsis *vte1* mutant exhibited delayed resistance to *Botrytis cinerea* infection (Cela et al., 2018). Furthermore, *VTE1* plays a substantial role in plant photoprotection by scavenging singlet oxygen and preventing lipid peroxidation (Ksas et al., 2018; Kumar et al., 2020; Rastogi et al., 2014). Notably, the function of *VTE1* in photoinhibition and photooxidative stress can be complemented by zeaxanthin and plastoquinone, suggesting a synergistic interplay amongst various photoprotective mechanisms within the plant (Havaux et al., 2005; Yao et al., 2015).

Here, we report the function of *HaVTE1* in sunflowers under abiotic stresses. We commenced with the identification and comparative analysis of VTE1 across 155 species, confirming its high degree of evolutionary conservation. The gene expression profiling revealed that *HaVTE1* expression levels varied in a tissue-specific manner and altered throughout different growth phases. Furthermore, promoter analysis, RNA-sequencing, and qRT-PCR suggested that *HaVTE1* may be involved in the MeJA and ABA signaling pathways. ABA is best known for its vital role in abiotic stress, causing stomatal closure and thereby enhancing plant stress resistance. (Hewage et al., 2020; Nakashima and Yamaguchi-Shinozaki, 2013).

To corroborate this, we generated *HaVTE1* overexpression lines in Arabidopsis, and hormone treatment confirmed that overexpression of *HaVTE1* can enhance resistance to MeJA and ABA. We further elucidated the function of *HaVTE1* in the ABA pathway by transgenic sunflower and subsequent transcript analysis. The results further strengthened that *HaVTE1* reduced the sensitivity to ABA by disturbing the upstream of the ABA signaling pathway and by facilitating the reduction of superoxide levels. Collectively, these findings provide a substantial groundwork for the continued exploration of *HaVTE1*'s molecular mechanism in mediating the ABA response in sunflowers.

2. Materials and methods

2.1. Phylogenetic analysis of the TC enzyme across diverse species

To elucidate the evolutionary relationships of the tocopherol cyclase (TC) enzyme among various species, 201 TC protein sequences were retrieved from NCBI (https://www.ncbi.nlm.nih.gov/). Before the next analysis, we screened using BLAST alignment and removed the redundant sequences. Subsequently, a total of 155 sequences remained and then integrated into a fasta. format file by Fasta Merge and Split procedure of TBtools (Chen et al., 2020). The dataset was subjected to multiple sequence alignments using the MUSCLE algorithm to ensure accurate homology assessment. Then, MEGA11 was employed to build the Neighbor-Joining tree (Kumar et al., 2016). We refined the phylogenetic tree in terms of the type of tree (radiation) and the branching order based on the plant evolution process. After optimizing, a file with nwk. format was obtained, which was used to visualize on the Interactive Tree of Life (iTOL) web platform (https://itol.embl.de/) (Han et al., 2022). Based on the plant classification, different colors were employed to represent responding Family or Genus. All the pictures showing the phylogenetic tree were downloaded on the internet.

2.2. Structure analysis of TC enzyme

The conserved motif of the full length of TC proteins was analyzed using the Motif Discovery-MEME section on the Multiple Em for Motif Elicitation (MEME) website (https://meme-suite.org/meme/). The parameters for calculating the motif procedure were the default settings provided by version 5.5.5, except for the number of searchable motifs, ten instead of three (Bailey et al., 2015). The Batch CD-search (https://www.ncbi.nlm.nih.gov/Structure/bwrpsb/bwrpsb.cgi), a tool belonging to Conserved Domain Database (CDD) which is part of Domains and Structures resource in NCBI, was employed to elucidate the conserved domain architecture of TC proteins (Lu et al., 2020). The MAST.xml file produced by the MEME website and the CDD HitData.txt file exported by the NCBI database were required to visualize the conserved motifs and domain of TCs. The kit named Gene Structure View in TBtools was employed to integrate all the results, including the Newick tree String. Additionally, the three-dimensional (3D) structural models of the TC enzyme were predicted and analyzed by SWISS-MODEL (https://swissmodel.expasy.org/) (Waterhouse et al., 2018). Subsequently, the above 3D models were subjected to pairwise structure alignment using online website RCSB PDB (https://www.rcsb.org/alignment) (Burley et al., 2022).

2.3. Promoter analysis of VTE1 across 28 representative species

The promoter sequences were sourced from the NCBI database. Most promoter regions were 2000 bp upstream from the transcription start site (ATG). The identification and computation of *cis*-acting regulatory elements within these promoter sequences were accomplished using PlantCARE (https://bioinformatics.psb.ugent.be/webtools/plantcare/html/) (Lescot et al., 2002). *Cis*-acting regulatory elements involved in light response were removed. Meanwhile, the length of promoters was recorded in a file with text. format. The Simple Biosequence Viewer procedure of TBtools presented the distribution of cis-acting elements on the promoter.

2.4. RNA-sequencing (RNA-seq) analysis

To analyze the expression pattern of *HaVTE1* under various treatments, public raw RNA-Sequencing data of sunflowers upon various treatments was downloaded from the NCBI Sequence Read Archive (SRA) database (Badouin et al., 2017). A plugin named "Kallisto Super Wrapper" in TBtools (v1.051) was employed to process the data. After inputting the transcript data, all the parameters are set to default. Then,

the TPM of *HaVTE1* was extracted from the resultant RNA sequencing data. Heatmap was performed by TBtools-II(v2.118).

To explore the mechanism of *HaVTE1* conferring plants ABA tolerant, RNA-seq analysis was performed with aerial tissues of empty vector (EV) and *HaVTE1* overexpression lines of sunflower with or without ABA treatment for 10 days. Each sample condition was replicated in triplicate to ensure the consistency and reliability of the transcriptomic data. Differentially expressed genes (DEGs) were identified using TBtools-II(v2.118), with criteria for significant differential expression established by |log2 (fold change)| >1, coupled with a *p*-value threshold of <0.05. Meanwhile, Gene Ontology (GO) analysis was performed by TBtools-II(v2.118). The visual presentation of the RNA-seq results was generated with bioinformatics (https://www.bioinformatics.com.cn/) and TBtools-II(v2.118).

2.5. Plant materials and growth conditions

The plants employed in the experiments were cultivated under controlled environmental conditions. AZB, a sunflower inbred line, was grown at 26–28 °C with 16 h light (150 μmol m^{-2} s^{-1}) / 8 h dark cycles. The sunflowers (without transgenic) were used for conducting the tissue-expression pattern of *HaVTE1* and hormone treatments were cultivated in soil. After germination on moist tissue, the transgenic sunflowers were transformed into 1 mL-tip boxes with 1/5 Hoagland Nutrient Solution (PHYGENE). Meanwhile, *Arabidopsis thaliana* (ecotype Columbia-0) and *Nicotiana benthamiana* were maintained at 21–23 °C with 16 h light (150 μmol m^{-2} s^{-1}) / 8 h dark cycles and 24–25 °C with 16 h light (100 μmol m^{-2} s^{-1}) /8 h dark cycles, respectively. Besides, Arabidopsis was planted in the 1/2 MS medium, while *Nicotiana benthamiana* was in the soil.

To detect the expression profile of *HaVTE1* in sunflowers, tissue samples were collected across 5 developmental stages and 6 seed stages of sunflowers with normal growth status, which were then subjected to qRT-PCR analysis. The 5 developmental stages included the germination stage (only cotyledon), seedling stage I (a pair of euphylla), seedling stage II (four pairs of euphylla), bud stage (the bud appeared and is no longer enlarged), and flowering stage (the tubiform florets are in full bloom). Besides, the tubiform florets were split into stigma, style, stamen, corolla, sepal, over and receptacle. 5 days after the flowering stage, seeds were sampled every week and lasted for 6 weeks. These samples were named I to VI according to the sampling order.

2.6. Hormone treatments

To investigate the modulation of ABA and MeJA on *HaVTE1* gene expression, 4-week-old AZB seedlings were subjected to hormone treatments. Roots of sunflowers were washed and soaked in water supplemented with 200 μM MeJA (Macklin, Shanghai, China) or 50 μM ABA (Macklin, Shanghai, China). Subsequent sampling of leaves and roots was carried out at 0, 1, 2, and 4 hours post-MeJA treatment and 0, 3, 6, and 9 hours following ABA treatment, encompassing both treated and control groups. Three biological replicates were performed in the above experiments.

For MeJA and ABA response assays, seeds from the WT and T_3 generation transgenic homozygous (#16 and #18) Arabidopsis were surfaced-sterilized by 75 % ethanol and 50 % bleach and subsequently sown on half-strength Murashige and Skoog (1/2 MS) medium for 5 days. Then, 15 seedlings with equal growth (root length = 1.0 cm) were transferred to fresh vertical 1/2 MS plates (with or without MeJA and ABA, respectively) by tweezers. The parameters such as leaf area and the number of lateral roots were measured and photographed after 12 days of cultivation. Three biological replicates were performed. The quantitative assessments of leaf blade area and lateral root number were facilitated by Image J (Schneider et al., 2012).

For assessments involving sunflower seedlings (both overexpression lines and gene-silenced lines), 10-day-old seedlings were cultured in 1/5 Hoagland nutrient solution (pH 5.8–6.0) supplemented with or without 50 μM ABA for 10 days.

2.7. Plasmid construction and plant transformation

To generate *p35S: HaVTE1-FLAG/GFP* constructs, full-length CDS of *HaVTE1* was amplified using the primer sets Flag/GFP-HaVTE1-F/R and then recombined into a binary vector pCD3–688-Flag/GFP with the *BamH*I site (Table S2). *p35S:HaVTE1-FLAG* was used for *HaVTE1* overexpression in Arabidopsis and sunflowers, and *p35S:HaVTE1-GFP* was used for subcellular localization in tobacco.

To generate the *HaVTE1-VIGS* vector, the specific 400 bp fragment of *HaVTE1* CDS was amplified using the primer sets TRV-HaVTE1-F/R with *BamH*I and *EcoR*I linker and then recombined into a binary pTRV2 vector (digested by *BamH*I and *EcoR*I). pTRV-*HaVTE1* plasmid was used to silence *HaVTE1* in sunflowers. These resulting vectors were transformed into *Agrobacterium tumefaciens* strain GV3101 for further transgenic processing.

The transient transformation of tobacco was carried out by leaf disc infection. After two days of incubation, the fluorescence signal in the leaves was detected with a confocal fluorescence microscope (Zeiss, Germany).

The transformation of Arabidopsis plants was performed by floral dip. The T_0 transgenic plants were selected on 1/2 MS medium containing 0.002 % basta (Coolaber, Beijing, China). Seeds from each T_0 plant were individually collected. Selected T_1 plants were propagated, and overexpression lines were confirmed by RT–PCR analysis. The primers used in this assay are listed in Table S2.

The transient transformation of sunflower (*Helianthus annuus*) plants was executed by employing seed-soak agroinoculation (SSA) (Jiang et al., 2021). The external and internal seed coats were removed, and then the seeds were soaked in sterile water for 1–2 days for sterilization and seed germination. The seeds were scraped with a sterile tweezer evenly and gently to facilitate inoculation. The wounded seeds were immersed in the inoculation solution with *Agrobacterium tumefaciens* harboring the appropriate genetic construct, 10 mM MES, 10 mM $MgCl_2$, 200 μM Acetosyringone (AS) and 5 % sucrose for 6 h in darkness at 28°C. Subsequently, the seeds and inoculation buffer were vacuumed together by a vacuum pump three times for 5 minutes. The infected seeds were put on the moist tissue for germination. Overexpression or silencing lines were confirmed by RT–PCR analysis and western blot.

2.8. RNA extraction, quantitative real-time-PCR (qRT-PCR) assay and immunoblot analysis

For expression analysis of *VTE1*, the total RNA of sunflower and Arabidopsis was extracted using RNAprep Pure Plant Kit (Tiangen, Beijing, China). 1.2 μg of total RNA was used for reverse transcription with HiScript II SuperMix Kit (Vazyme, Nanjing, China). The qRT-PCR analysis was conducted on the CFX384 detection system (BIO-RAD, CA, USA) using ChamQ Master Mix (Vazyme, Nanjing, China) according to the manufacturer's instructions. The experiments were executed with three independent biological replicates. Three technical replicates were performed. The *HaTublin* gene was employed as an internal control. $2^{-\triangle\triangle CT}$ method was used to compute gene relative expression level. The qRT-PCR primers used in this assay were listed in Table S2.

For immunoblot analysis of VTE1, the total protein was extracted from leave tissues resuspended with protein extraction buffer (50 mM of Tris–HCl at pH 8.0, 150 mM of NaCl, 10 mM of $MgCl_2$, 1 mM of EDTA, 10 % (v/v) glycerol, and Protease inhibitor cocktail). The mixture was incubated at 4℃ for 30 min with rotation and then centrifugation at 12, 000 g for 10 min at 4℃. The supernatant was added with 5×SDS loading buffer and boiled at 98℃ for 8 min. The extracted proteins were finally separated in 10 % SDS-PAGE gels and detected by western blot analysis using anti-VTE1 (PHY3414A, PHYTOAB, 1:1000).

2.9. Measurement of the water loss rate of leaf and ROS

The water loss rate of leaves was assessed in detached rosette leaves of 4-week-old plants. The leaves were weighed every 5 min for 1 h, in triplicate. The percentage loss of fresh weight was calculated based on the initial weight of the leaves.

7-day-old seedlings of Col-0 and *HaVTE1* overexpression lines #16 and #18 ($n = 4$) were treated in ddH_2O with or without 50 μM ABA for 3 h before the seedlings were stained. To visualize superoxide accumulation, the seedlings were incubated in 1.0 $mg{\cdot}mL^{-1}$ NBT (Sigma-Aldrich) dissolved in 25 mM HEPES buffer (pH 7.6) buffer for 20–30 min (Arabidopsis) and overnight (sunflower) in darkness at room temperature. The seedlings stained by NBT were then washed with 95 % ethanol until chlorophyll in the leaves faded and photographed.

Images of roots for ROS staining were performed utilizing a Nikon ECLIPSE 80i light microscope. Average NBT intensity and relative area of NBT stain were measured with three biological replicates using Image J.

2.10. Luciferase activity detection

To assess the effect of ABA pathway genes on VTE1, the promoters (about 1.5 Kb) of 6 ABA pathway genes (*LOC110884474*, *LOC110880238*, *LOC110912722*, *LOC110885370*, *LOC110894640*, *LOC110889853*) were amplified and cloned into pGreen-0800-LUC to generate *pHaPYL4: LUC*, *pHaPP2C: LUC*, *pHaSnRK2: LUC*, *pHaABIL5: LUC* reporter constructs. The *p35S: HaVTE1-FLAG* was generated for effector construct. The recombinant plasmids were transferred to the Agrobacterium *EHA105* strain. The combined reporter and effector bacteria were resuspended with infecting buffer (10 mM MES [pH5.7], 10 mM $MgCl_2$, and 0.2 mM AS) for 1 hour, and then injected into the young leaves of tobacco (*N. benthamiana*). After three days of infiltration, the leaves were coated with luciferin (E1601, Promega) and kept in the dark for 10 min to quench autofluorescence. The luciferase activity was captured using the PlantView100 assay system (BLT Photon Technology). All of the experiments were independently repeated at least three times. The primers used are listed in Table S2.

2.11. Statistical analysis

All statistical analyses were performed by the Student's *t*-test or two-way ANOVA test in the SPSS application. Asterisk represent statistical significance ($^*P < 0.05$, $^{**}P < 0.01$, and). a, b and c indicate significant differences by two-way ANOVA ($p < 0.01$). All the graphical representations were generated with GraphPad Prism 9.

3. Results

3.1. The conservative structures of VTE1

To explore the diversity and evolutionary characteristics of the VTE1/TC in different organisms, a total of 155 protein sequences were identified and retrieved from NCBI, including 145 *Viridiplantae* representative species (including algae, bryophytes, ferns and angiosperm, as cataloged in Table 1 and Table S1) and 10 outgroup members (archaea and lower marine animal). Therein, the VTE1 sequences had a range from 323 to 528 amino acid residues (aa). The grand average of hydropathicity spanned from −0.638 to −0.064, suggesting general neutrality in terms of hydrophilicity among the VTE1/TC proteins analyzed. These bioinformatic analyses offer valuable insights into the variable characteristics exhibited by the VTE1/TC proteins.

To elucidate the genetic phylogeny of *VTE1*, the dataset comprising 155 VTE1 sequences was employed to construct a phylogenetic tree by MEGA11 (Fig. 1). Among green plants, 145 species can be categorized into two major groups: algae and land plants. Within the angiosperm clade, the monocots and eudicots formed two distinct evolutionary branches. Remarkably, the VTE1 of eudicots displayed four lineages. The first lineage comprised 12 families, including Asteraceae and Solanaceae. The prominent features of the second lineage are members of the legume and gourd families. The third and fourth lineages incorporated families such as Rosaceae and Juglandaceae, and Brassicaceae and Malvaceae, respectively. In summary, the phylogenetic analysis of VTE1/TCs demonstrated a highly conservative in evolution.

To investigate the structural evolution of the VTE1s, we analyzed the conserved motifs and domains across the VTE1 sequences of 155 species (Fig. S1). A total of 10 different motifs were identified (Fig. S2). Notably, motif 7 was first formed, suggesting that it was essential to the functional integrity of VTE1. Compared with archaea, more conserved motifs, such as motifs 5 and 4, were further formed in algae. Nonetheless, the order of motifs appeared rather disorderly and lacked uniformity. Bryophytes VTE1/TCs further formed motif 9, representing the incipient formation of a more complex molecular architecture. Upon evaluating the fern VTE1/TCs, we observed that the number and sequence of conserved motifs mirrored those found in angiosperms, implying a significant degree of evolutionary conservation across these lineages. The appearance and disappearance of motifs are examples of the diversity of VTE1 proteins. Specific instances of such evolutionary changes include the generation of a novel motif 7 in several species of the genus Solanum, the introduction of motif 10 in *Macadamia integrifolia*, and motif 5 in *Salvia hispanica*; as well as alterations in *Ziziphus jujuba* and *Zea mays* involving motifs 7 and 9, and motif 3, respectively.

Although there are significant differences in the amino acid sequences of TC in archaea, algae, and terrestrial plants, their three-dimensional structures were similar (Fig. 2 and Fig. S3). The visible differences among them were the relative positions of the β-sheets (Fig. 2).

3.2. The expression pattern and subcellular localization of HaVTE1

To elucidate the expression pattern of *VTE1* in sunflowers, we analyzed a range of tissues across 5 stages, encompassing the germination stage, two seedling stages (I and II), the bud stage, the flowering stage, and the seed stage. Total RNA was extracted from samples and quantitative reverse transcription-PCR (qRT-PCR) was employed to profile the expression of *HaVTE1* (Fig. 3A and Fig. S4). The results revealed that *HaVTE1* was ubiquitously expressed across samples with notably elevated expression in leaves during vegetative growth (Fig. 3A). Interestingly, a shift in the pattern of abundant *HaVTE1* expression was observed during the transition from vegetative to reproductive growth. Additionally, *HaVTE1* had a higher transcript level in the seed stage II (Fig. S4). To further characterize the subcellular localization of HaVTE1, the GFP-tagged HaVTE1 vector was constructed and transformed to agrobacterium, and instantaneously converted into *Nicotiana benthamiana* leaves using the leaf dish transformation method. As shown in Fig. 3B, GFP signals were detected in the chloroplast, which was consistent with its role as the enzyme of VTE synthesis (Fig. 3B).

3.3. Sunflower HaVTE1 was induced by ABA and MeJA

To further explore the potential roles of *VTE1* in sunflowers, an investigation was conducted focusing on the *cis*-regulatory elements within the promoters of *VTE1* genes from 28 representative species (Fig. S5). We found that MeJA and ABA response elements appeared most frequently by counting the types number of response elements on promoters. Particularly notable were several MeJA and ABA-responsive elements located on the promoter of *HaVTE1* (Fig. 4A). To extend these insights, we conducted publicly available RNA-sequencing (RNA-seq) data from sunflowers subjected to various treatments, and *HaVTE1* expression was found to be up-regulated in leaves and roots upon exposure to ABA (Fig. 4B). To validate these findings, qRT-PCR expression assays were conducted in sunflowers treated with ABA and MeJA. As shown in Fig. 4C, the assays confirmed both hormones'

Table 1
The characteristics of TCs in 155 species.

ID	Species	Number of Amino Acid	MW (Da)	PI	Instability Index	Aliphatic Index	Grand Average of Hydropathicity
WP_002796597.1	*Microcystis aeruginosa*	353	40278.63	7.07	31.56	74.62	−0.326
WP_011032471.1	*Methanosarcina mazei*	329	37095.57	9.12	22.76	76.75	−0.266
XP_038985009.1	*Phoenix dactylifera*	492	54359.53	6.25	47.84	64.07	−0.312
XP_030482476.1	*Cannabis sativa*	503	56337.42	6.55	47.18	61.63	−0.473
XP_020149175.1	*Aegilops tauschii subsp. strangulata*	467	52088.74	7.1	43.33	58.95	−0.466
XP_010447345.1	*Camelina sativa*	486	54384.22	5.9	41.54	64.79	−0.386
XP_043704082.1	*Telopea speciosissima*	521	58315.42	6.44	44.09	64.91	−0.451
XP_043606699.1	*Erigeron canadensis*	518	58255.48	8.28	37.04	65.83	−0.533
NP_567906.1	*Arabidopsis thaliana*	488	54720.67	5.95	49.22	66.52	−0.409
XP_025623799.1	*Arachis hypogaea*	456	51304.8	6.05	50.48	63.75	−0.407
XP_044464352.1	*Mangifera indica*	497	55520.45	6.06	46.56	64.55	−0.364
XP_015945681.1	*Arachis duranensis*	456	51331.87	6.22	50.48	63.75	−0.414
XP_021687411.1	*Hevea brasiliensis*	508	56997.36	7.16	38.36	65.04	−0.384
NP_001291340.1	*Sesamum indicum*	494	55750.19	6.07	40.41	65.14	−0.369
XP_035814736.1	*Zea mays*	451	50057.43	6.05	48.02	68.51	−0.343
XP_020518284.1	*Amborella trichopoda*	512	57282.61	5.79	37.59	67.25	−0.326
XP_022131899.1	*Momordica charantia*	515	57982.44	6.49	48.3	64.39	−0.459
XP_024358058.1	*Physcomitrium patens*	451	50591.08	5.26	40.18	61	−0.431
XP_030946713.1	*Quercus lobata*	503	56154.4	7.11	46.34	69.2	−0.385
XP_038884980.1	*Benincasa hispida*	528	59326.88	6.66	41.88	62.78	−0.482
XP_039143052.1	*Dioscorea cayenensis subsp. rotundata*	466	52136.94	6.33	50.73	67.17	−0.321
XP_020218342.1	*Cajanus cajan*	483	54197.2	6.16	46.44	68.05	−0.355
XP_010234137.1	*Brachypodium distachyon*	471	52169	6.48	44.75	65.22	−0.354
NP_001310379.1	*Solanum pennellii*	498	55678.76	6.25	41.2	66.75	−0.373
XP_003522704.1	*Glycine max*	489	54941.89	5.74	41.96	65.6	−0.405
XP_002176411.1	*Phaeodactylum tricornutum CCAP*	515	58496.46	9.05	40.23	70.06	−0.369
XP_010915874.1	*Elaeis guineensis*	492	54015	6.16	45.24	66.44	−0.258
XP_020692111.1	*Dendrobium catenatum*	485	54094.22	8.02	41.26	63.55	−0.351
XP_024166545.1	*Rosa chinensis*	490	54701.61	6.52	45.47	63.1	−0.446
XP_028228222.1	*Glycine soja*	489	54921.88	5.86	41.87	65.6	−0.412
XP_038700291.1	*Tripterygium wilfordii*	500	55595.55	6.48	39.11	68.42	−0.41
XP_042469545.1	*Zingiber officinale*	497	55150.15	6.34	42.25	64.16	−0.312
XP_002516548.1	*Ricinus communis*	505	56620.65	5.64	44.6	63.52	−0.426
XP_002291625.1	*Thalassiosira pseudonana CCMP1335*	448	51281.54	6.45	50.56	62.05	−0.545
XP_009413813.1	*Musa acuminata subsp. malaccensis*	499	55146.2	6.44	46.6	65.49	−0.307
XP_021739186.1	*Chenopodium quinoa*	505	56618.74	5.86	54.11	64.48	−0.41
XP_022754591.1	*Durio zibethinus*	506	56858.21	6.58	47.85	64.78	−0.365
XP_034201471.1	*Prunus dulcis*	491	55100.01	6.74	46.33	64.34	−0.479
XP_034893466.1	*Populus alba*	501	55965.98	6.29	44.4	65.99	−0.376
XP_016180783.1	*Arachis ipaensis*	456	51277.75	5.97	50.28	63.11	−0.4
XP_013462012.1	*Medicago truncatula*	479	53782.58	6.34	42.72	63.34	−0.412
XP_002971673.1	*Selaginella moellendorffii*	453	50297.71	5.99	46.56	65.43	−0.342
XP_015626329.1	*Oryza sativa*	470	52194.84	6.81	47.45	61.87	−0.407
XP_005651298.1	*Coccomyxa subellipsoidea C−169*	483	53132.56	6.87	41.8	70.31	−0.365
XP_011396277.1	*Auxenochlorella protothecoides*	393	42652.2	6.8	40.88	71.7	−0.247
XP_022783187.1	*Stylophora pistillata*	386	42511.02	5.3	29.15	77.8	−0.092
XP_007515274.1	*Bathycoccus prasinos*	490	54182.34	5.64	45.89	63.88	−0.513
XP_005702972.1	*Galdieria sulphuraria*	451	52519.7	8.21	47.94	72.57	−0.365
XP_022838185.1	*Ostreococcus tauri*	483	51960.02	5.66	40.11	71.76	−0.286
XP_006450664.1	*Citrus clementina*	476	53772.63	6.87	44.65	64.92	−0.41
XP_010254049.1	*Nelumbo nucifera*	523	58754.18	6.85	44.42	66.58	−0.44
XP_012077416.1	*Jatropha curcas*	501	56706.81	6.9	41.78	62.26	−0.445
XP_012436456.1	*Gossypium raimondii*	527	58478.2	6.53	46.64	69.39	−0.251
XP_021978512.1	*Helianthus annuus*	483	53934.88	6.68	35.71	68.82	−0.397
XP_016681625.2	*Gossypium hirsutum*	528	58725.54	7.49	49.15	68.88	−0.259
XP_031373715.1	*Punica granatum*	503	56214.02	6.4	49.23	61.65	−0.443
XP_044973580.1	*Hordeum vulgare subsp. vulgare*	469	52259.91	6.87	44.78	58.91	−0.466
XP_042992370.1	*Carya illinoinensis*	512	57312.46	6.25	43.46	65.12	−0.388
XP_044331917.1	*Triticum aestivum*	468	52322.99	6.77	42.18	59.44	−0.462
XP_018842576.1	*Juglans regia*	512	57045.22	8.03	42.98	63.98	−0.391
XP_002281424.1	*Vitis vinifera*	502	56519.53	6.25	44.56	63.13	−0.433
NP_001274927.1	*Solanum tuberosum*	501	56214.14	5.8	44.47	64.79	−0.397
WP_156092401.1	*Mycobacterium ulcerans*	333	36462.65	5.61	28.66	76.07	−0.246
XP_038075659.1	*Patiria miniata*	402	43942.8	5.27	39.28	77.59	−0.064
WP_013644668.1	*Methanobacterium lacus*	327	37701.29	7.67	29.66	80.21	−0.287
WP_012955234.1	*Methanobrevibacter ruminantium*	355	41160.79	5.64	35.19	60.48	−0.638
XP_006283540.2	*Capsella rubella*	493	55257.25	5.84	44.87	64.85	−0.408
XP_042498327.1	*Macadamia integrifolia*	519	58233.29	6.54	45.83	63.89	−0.434
XP_042039337.1	*Salvia splendens*	494	55205.39	7.01	42.27	63.2	−0.413
XP_041021112.1	*Juglans microcarpa x Juglans regia*	512	57014.17	7.08	44.62	64.16	−0.379
XP_039789080.1	*Panicum virgatum*	481	52632.34	5.97	47.61	64.1	−0.334

(*continued on next page*)

Table 1 (*continued*)

ID	Species	Number of Amino Acid	MW (Da)	PI	Instability Index	Aliphatic Index	Grand Average of Hydropathicity
XP_039031821.1	*Hibiscus syriacus*	503	56628.95	6.25	44.91	63.02	−0.377
XP_037413002.1	*Triticum dicoccoides*	468	52322.99	6.77	42.18	59.44	−0.462
XP_034683432.1	*Vitis riparia*	502	56559.54	6.25	44.35	64.28	−0.432
XP_031486043.1	*Nymphaea colorata*	481	53950.53	6.19	52.54	69.71	−0.258
XP_031256610.1	*Pistacia vera*	524	58095.43	6.57	43.84	62.14	−0.336
XP_031101652.1	*Ipomoea triloba*	487	54453.2	6.73	43.96	62.07	−0.487
XP_030452636.1	*Syzygium oleosum*	520	57579.64	8.27	53.07	59.12	−0.458
XP_028095320.1	*Camellia sinensis*	503	56590.03	8.41	40.89	64.73	−0.443
XP_027904295.1	*Vigna unguiculata*	482	54076.97	5.66	43.09	64.94	−0.412
XP_026447744.1	*Papaver somniferum*	507	56681.87	6.49	39.72	65.01	−0.42
XP_025807988.1	*Panicum hallii*	476	52397.25	6.48	42.56	66.85	−0.287
XP_023904572.1	*Quercus suber*	505	56522.84	7.14	45.33	68.73	−0.398
XP_023758644.1	*Lactuca sativa*	506	56758.03	6.49	36.05	67.41	−0.433
XP_023538605.1	*Cucurbita pepo subsp. pepo*	515	57810.26	8.38	45.02	62.12	−0.468
XP_023002310.1	*Cucurbita maxima*	515	57601.86	6.62	42.78	62.87	−0.437
XP_022951773.1	*Cucurbita moschata*	515	57847.24	7.95	43.17	62.12	−0.471
XP_022865376.1	*Olea europaea var. sylvestris*	474	52631.38	6.5	38.17	62.95	−0.39
XP_021835572.1	*Spinacia oleracea*	507	56633.75	5.77	48.02	62.5	−0.418
XP_021819281.1	*Prunus avium*	491	55033.77	7.12	47.77	62.75	−0.513
XP_021597420.1	*Manihot esculenta*	508	56934.9	6.17	48.7	61.06	−0.446
XP_021277348.1	*Herrania umbratica*	509	56792.04	7.61	44.99	63.81	−0.381
XP_020581775.1	*Phalaenopsis equestris*	485	54074.22	6.57	40.08	66.78	−0.312
XP_020243063.1	*Asparagus officinalis*	414	46767.67	8.04	49.76	61.01	−0.487
XP_020097304.1	*Ananas comosus*	476	52804.57	6.48	43.25	66.83	−0.344
XP_017411915.1	*Vigna angularis*	488	54651.69	5.65	45.92	66.56	−0.397
XP_014501691.1	*Vigna radiata var. radiata*	492	55289.53	5.65	45.31	68.01	−0.352
XP_013719625.1	*Brassica napus*	490	54920.63	6	48.5	59.14	−0.482
XP_013593603.1	*Brassica oleracea var. oleracea*	490	55031.79	6.26	47.65	59.53	−0.501
XP_012857904.1	*Erythranthe guttata*	494	55279.66	8.36	35.05	62.39	−0.435
XP_011026617.1	*Populus euphratica*	501	56077.29	6.14	44.57	67.92	−0.327
XP_010049096.2	*Eucalyptus grandis*	515	56826.82	7.11	47.68	61.96	−0.417
XP_009770568.1	*Nicotiana sylvestris*	513	57433.71	6.77	39.87	64.64	−0.408
XP_009604121.1	*Nicotiana tomentosiformis*	513	57594.16	7.95	40.6	67.47	−0.396
XP_009367893.1	*Pyrus x bretschneideri*	486	54567.21	6.06	49.21	62.02	−0.507
XP_009138143.1	*Brassica rapa*	490	54884.53	5.95	48.59	58.35	−0.486
XP_008445022.1	*Cucumis melo*	517	57788.19	6.81	40.59	65.82	−0.415
XP_008393882.2	*Malus domestica*	486	54431.09	5.94	50.13	63	−0.474
XP_008220061.1	*Prunus mume*	491	55118.88	6.74	46.33	61.96	−0.517
XP_015688553.2	*Oryza brachyantha*	463	51191.47	5.91	44.85	60.73	−0.432
XP_006476062.1	*Citrus sinensis*	476	53904.86	7.64	45.12	64.1	−0.424
XP_004952221.1	*Setaria italica*	480	52575.23	6.53	48.11	67.1	−0.29
XP_004501172.1	*Cicer arietinum*	483	54195.05	6.23	41.48	64.64	−0.377
XP_004291189.1	*Fragaria vesca subsp. vesca*	484	54239.19	6.88	38.48	62.5	−0.464
XP_004245276.1	*Solanum lycopersicum*	498	55579.68	6.12	41.48	67.15	−0.35
XP_011649737.1	*Cucumis sativus*	517	57822.05	6.41	41.72	63	−0.471
XP_024023844.1	*Morus notabilis*	502	56439.38	6.69	43.35	59.8	−0.466
XP_007222342.1	*Prunus persica*	491	55108.96	6.74	47	63.54	−0.503
XP_006371708.2	*Populus trichocarpa*	501	55976.91	5.83	45.43	66.57	−0.362
XP_006412433.1	*Eutrema salsugineum*	494	55220.13	6.36	46.98	62.19	−0.417
XP_020874882.1	*Arabidopsis lyrata subsp. lyrata*	482	54054.9	6.4	44.83	65.33	−0.428
XP_002453692.1	*Sorghum bicolor*	475	52300.05	6.12	47.45	67.18	−0.28
XP_047325740.1	*Impatiens glandulifera*	493	55467.7	6.25	40.24	68.28	−0.348
XP_046556286.1	*Haliotis rubra*	368	40810.63	8.38	38.04	82.34	−0.089
XP_027354634.1	*Abrus precatorius*	464	52023.63	5.8	42.68	66.83	−0.39
XP_017629026.1	*Gossypium arboreum*	508	56591.01	7.93	49.49	67.19	−0.334
XP_048331844.1	*Ziziphus jujuba var. spinosa*	474	53302.03	6.11	47.15	63.76	−0.452
XP_010668187.2	*Beta vulgaris subsp. vulgaris*	505	56241.2	5.68	52.61	62.18	−0.424
WP_260594462.1	*Salinirubellus salinus*	326	35972.56	4.75	33.7	73.25	−0.456
WP_255150549.1	*Halosegnis sp. ZY10*	323	35494.69	4.49	31.55	66.72	−0.528
XP_019255404.1	*Nicotiana attenuata*	513	57352.56	6.53	39.13	64.81	−0.397
XP_048535298.1	*Triticum urartu*	468	52322.99	6.77	42.18	59.44	−0.462
XP_045799464.1	*Trifolium pratense*	487	54752.64	6.24	38.71	63.7	−0.43
XP_019432256.1	*Lupinus angustifolius*	489	55062.16	7.13	39.76	66.79	−0.44
XP_051205974.1	*Lolium perenne*	468	51892.28	6.15	46.46	59.23	−0.482
XP_051151573.1	*Andrographis paniculata*	490	55208.43	6.73	38.06	64.47	−0.434
XP_050881088.1	*Pisum sativum*	491	54958.73	6.09	37	61.41	−0.446
XP_050266958.1	*Quercus robur*	503	56182.37	6.78	47.52	68.23	−0.398
XP_050212527.1	*Mercurialis annua*	499	56096.56	7.11	44.99	64.85	−0.378
XP_050127764.1	*Malus sylvestris*	486	54447.14	5.94	49.74	63.81	−0.463
XP_049377637.1	*Solanum stenotomum*	501	56156.15	5.94	45.14	65.57	−0.395
XP_049373826.1	*Solanum verrucosum*	502	56338.37	5.94	45.09	65.44	−0.385
XP_047974796.1	*Salvia hispanica*	494	55140.34	8.04	39.98	64.19	−0.422
XP_047150627.1	*Vigna umbellata*	488	54640.86	5.54	45.27	65.76	−0.39
XP_047081392.1	*Lolium rigidum*	472	52317.88	6.43	42.78	59.15	−0.465
XP_034588862.1	*Setaria viridis*	480	52516.16	6.34	48.11	67.1	−0.284

(*continued on next page*)

Table 1 (*continued*)

ID	Species	Number of Amino Acid	MW (Da)	PI	Instability Index	Aliphatic Index	Grand Average of Hydropathicity
XP_027180681.1	*Coffea eugenioides*	509	56907.17	6.54	45.87	60	−0.417
XP_027081567.1	*Coffea arabica*	509	56952.21	6.49	45.97	60	−0.421
XP_019183801.1	*Ipomoea nil*	487	54483.26	6.54	44.11	62.3	−0.472
XP_018480322.1	*Raphanus sativus*	491	54890.62	6.07	48.39	60.59	−0.475
XP_017255764.1	*Daucus carota subsp. sativus*	489	54980.94	7.59	48.03	64.83	−0.449
XP_016537987.2	*Capsicum annuum*	500	55831.03	6.11	40.83	67.28	−0.361
XP_016477244.1	*Nicotiana tabacum*	513	57586.09	7.55	40.01	66.71	−0.396
XP_013707373.2	*Brassica napus*	490	55031.79	6.26	47.65	59.53	−0.501
XP_007012099.2	*Theobroma cacao*	509	56764.95	6.81	47.34	63.81	−0.385

A

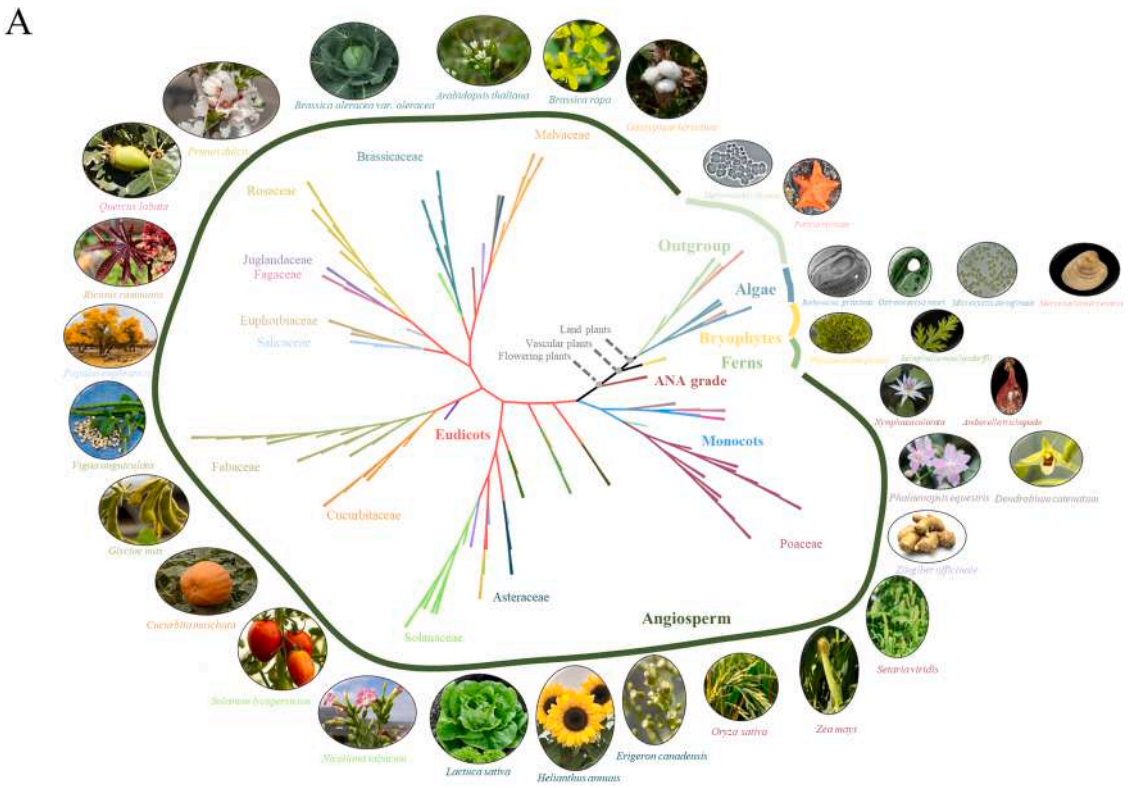

B

Type of plants	Number of Species
Outgroup	10
Algae	8
Bryophytes	1
Fern	1
Angiosperm	135
Total	155

Fig. 1. Phylogenetic relationships of VTE1 in 155 species. (A) The phylogenetic tree of VTE1 was constructed using Neighbor-Joining (NJ) methods by MEGA11 based on a concatenated sequence alignment of 155 single-copy genes downloaded from NCBI. There are 145 species (details can be seen in Table S1) and 10 outgroup members (the latter including Archaebacteria and some lower marine animals). Colored bars surrounding the tree represent recognized divisions (or phyla) of the green lineage: Algae, Bryophytes, Ferns, and Angiosperm which can be divided into ANA grade (2), monocots (25), and eudicots (108). Colors on branches reflect different taxonomic clades. All images were downloaded on the Internet. **(B)** The classification of 155 species.

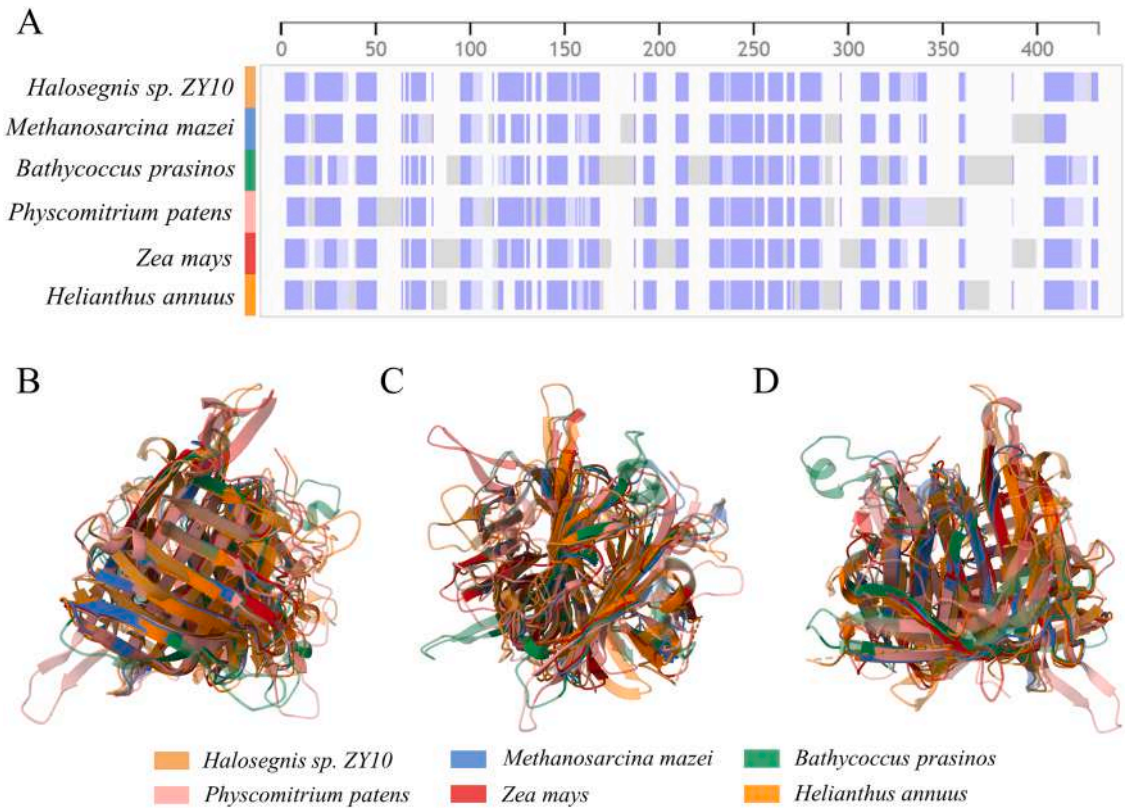

Fig. 2. Three-dimensional structure alignment of VTE1 in 6 representative species. (A) The diagram of VTE1 protein structure alignment. Different colours indicated corresponding species. The colours of Fig. 2A corresponded to that of Fig. 2B-D. **(B-D)** VTE1 Sequence alignment in 3D. Different colours indicated corresponding species. **(C)** and **(D)** were generated by rotating **(B)** counterclockwise by 90° and 180°, respectively.

significant induction of HaVTE1 expression. Collectively, these findings strongly suggested that *HaVTE1* was responsive to MeJA and ABA pathway.

3.4. Overexpression of HaVTE1 in Arabidopsis showed reduced sensitivity to MeJA and ABA

To elucidate the role of *HaVTE1* in stress response, an expression construct containing the full-length CDS of *HaVTE1* driven by 35S promoter was introduced into Arabidopsis. *HaVTE1*-OE lines showed significant differences in leaf development (Fig. S6). The number of leaves and bolting in *HaVTE1*-OE lines was remarkably higher than that of WT. To assess the role of *HaVTE1* on the response to MeJA and ABA, five-day-old seedlings of WT and *HaVTE1-OE* lines cultivated on 1/2 MS medium were transferred to fresh vertical plates with varying concentrations of MeJA or ABA. Specifically, the *HaVTE1* overexpression lines exhibited an increase in root proliferation and leaf expansion compared to WT plants, under MeJA treatment (Fig. S7).

For ABA treatment, transgenic Arabidopsis seedlings were treated with 15 μM and 30 μM ABA, respectively. *HaVTE1* overexpression lines exhibited marked improvements in growth compared to WT (Fig. 5A). Analyses of morphological features revealed that the leaf blade area of the *HaVTE1*-OE lines surpassed that of the WT in the presence of ABA (Fig. 5B), and a significant increase in the number of lateral roots was observed in the *HaVTE1*-OE lines relative to WT (Fig. 5C). To reveal the role of *HaVTE1* in ABA-mediated stomatal closure, the water loss rates from detached leaves were investigated. As shown in Fig. 5D, the results exhibited a higher rate of water loss in the detached leaves of the two *HaVTE1*-OE lines versus the WT, consistent with a reduced sensitivity to ABA-mediated stomatal closure in the overexpression lines.

The robust anti-oxidative capacities of *HaVTE1* have prompted hypotheses that it may act to mitigate reactive oxygen species (ROS) during ABA-induced stress responses. To corroborate this, ROS in leaves and roots of WT and *HaVTE1* overexpression plants under ABA treatment were detected by nitroblue tetrazolium (NBT) staining (Fig. 6). Results showed that the average ROS level of *HaVTE1*-OE was both less than WT (Fig. 6), which corresponded to the ABA insensitive phenotypes of *HaVTE1* overexpression lines. In conclusion, these results demonstrated that *HaVTE1* overexpression impaired ABA sensitivity.

3.5. HaVTE1 decreases sensitivity to ABA treatment in sunflowers

To substantiate the involvement of *HaVTE1* in the ABA pathway, we constructed transiently transformed sunflowers via *HaVTE1* overexpression and virus-induced gene silencing (VIGS). Then, the mRNA and protein level of *HaVTE1* in transgenic sunflowers was detected by qRT-PCR and western blot to confirm transformation efficiency (Fig. 7C-D). The *HaVTE1* transgenic sunflowers showed no significant difference compared with the control group, which harbored the transformed empty vector under normal conditions (Fig. 7A). When subjected to ABA treatment, two representative *HaVTE1* overexpression lines displayed a pronounced insensitivity compared to the control group Conversely, TRV-*HaVTE1* silenced lines exhibited increased sensitivity to ABA, as evidenced by diminished growth, smaller and more wilted true leaves, and the onset of necrosis in cotyledons (Fig. 7B).

Moreover, to directly visualize O_2^- accumulation under ABA treatment, we stained sunflower leaves sampled from the transgenic and EV lines with NBT. As shown in Fig. 7E-F, the NBT average intensity in *HaVTE1* leaves with or without ABA treatment was significantly lower than the control group, suggesting the strong oxidation resistance of *HaVTE1*. In contrast, the TRV-*HaVTE1* silenced lines exhibited greater oxidative damage. Collectively, these findings were consistent with the phenotypes of *HaVTE1*-OE lines in Arabidopsis lines and lend further support to the functional role of *HaVTE1* in mediating plant responses to

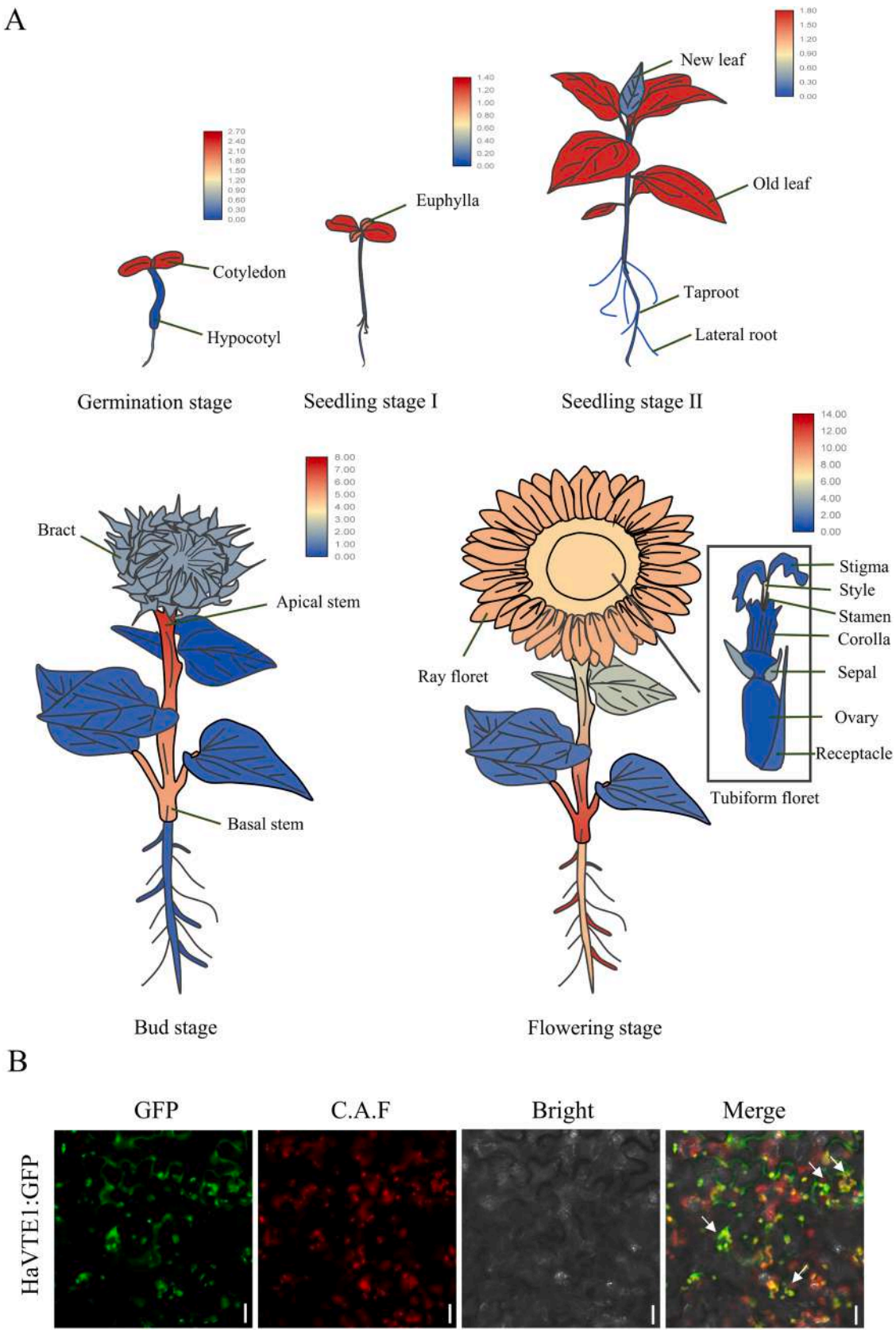

Fig. 3. Expression pattern and subcellular localization of *HaVTE1*. (A) Expression analysis of *HaVTE1* in different tissues at five stages (Germination stage, Seedling stage I, Seedling stage II, Bud stage, Flowering stage, and Seed stage). Tissues include cotyledon, hypocotyl, euphylla, taproot, lateral root, new leaf, old leaf, basal stem, apical stem, bract, ray floret, and tubiform floret. *HaTubulin* was used as a control. **(B)** Subcellular localization of HaVTE1-GFP fusion protein in the leaf epidermal cells of *N. benthamiana.* C.A.F = chloroplast autofluorescence. Bar = 20 μM.

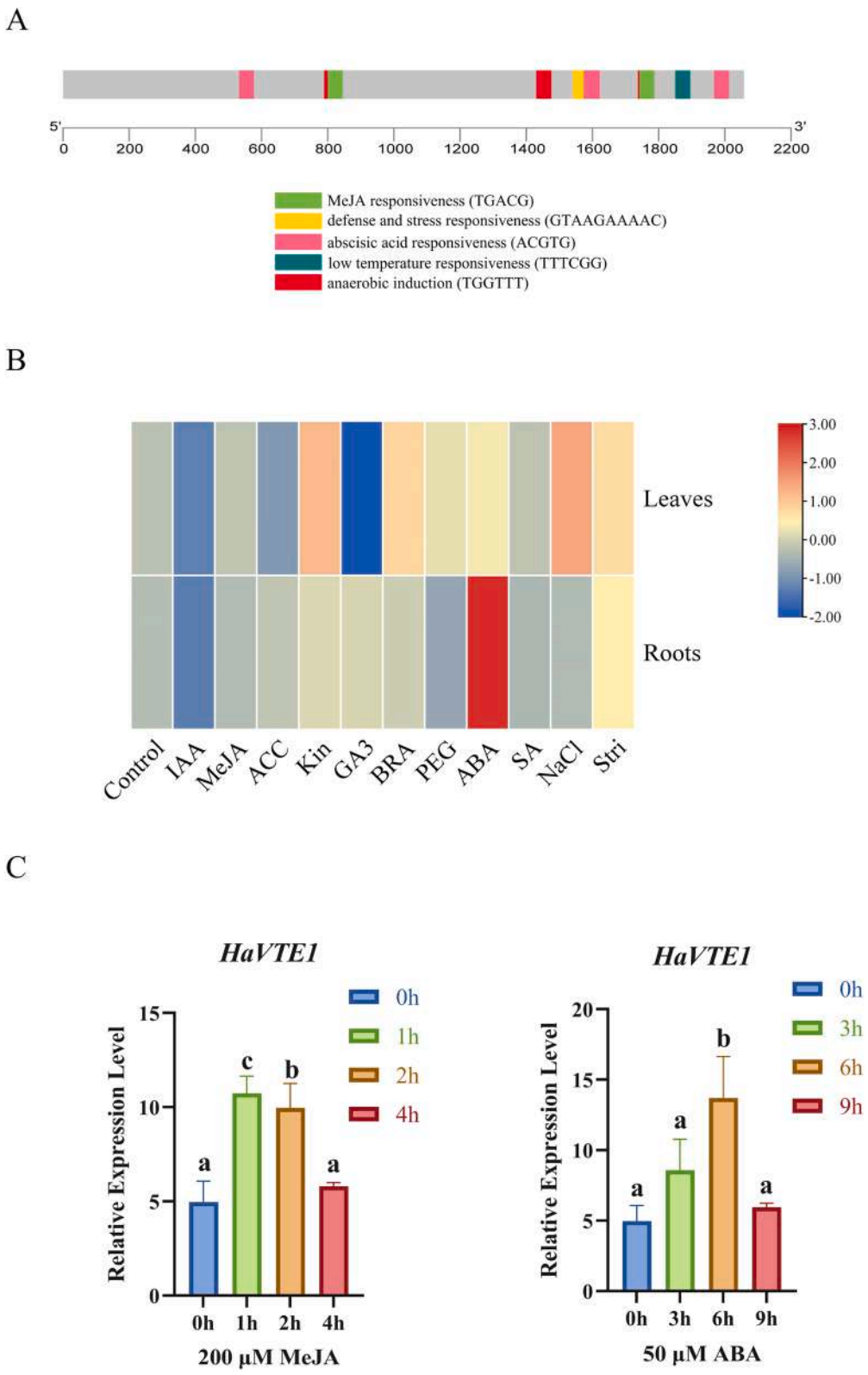

Fig. 4. Expression pattern of *HaVTE1* under different treatments in Sunflower. (A) Predicted *cis*-elements in *HaVTE1* promoters. Different colors represent the different types of *cis*-elements. More analysis of *VTE1* promoter elements in different species can be seen in Fig. S3. The contents in parentheses are concrete sequences of corresponding *cis*-elements. **(B)** The relative expression level of *HaVTE1* in response to various treatments. The data came from the NCBI public *RNA-seq* database and the heatmap was analyzed by TBtools. IAA, 0.1 μM 3-Indoleacetic acid; MeJA, 1 μM methyl jasmonate; ACC, 0.25 μM 1-aminocyclopropane-1-carboxylic acid; Kin, 0.5 μM kinetin; GA3, 10 μM gibberellic acid 3; BRA, 1 μM 24-epibrassinolide; PEG, 100 g/L polyethylene glycol 6000; ABA, 10 μM abscisic acid; Sa, 0.05 μM salicylic acid; NaCl, 100 mM sodium chloride; Stri, 0.1 μM rac-GR24, a strigolactone analog. **(C)** qRT–PCR analysis of *HaVTE1* expression of sunflower in response to MeJA and ABA. *HaTubulin* was used as a control. Each value is the mean ±SEM of three independent measurements. a, b and c indicate significant differences by two-way ANOVA ($p < 0.01$). Three biological replicates were performed.

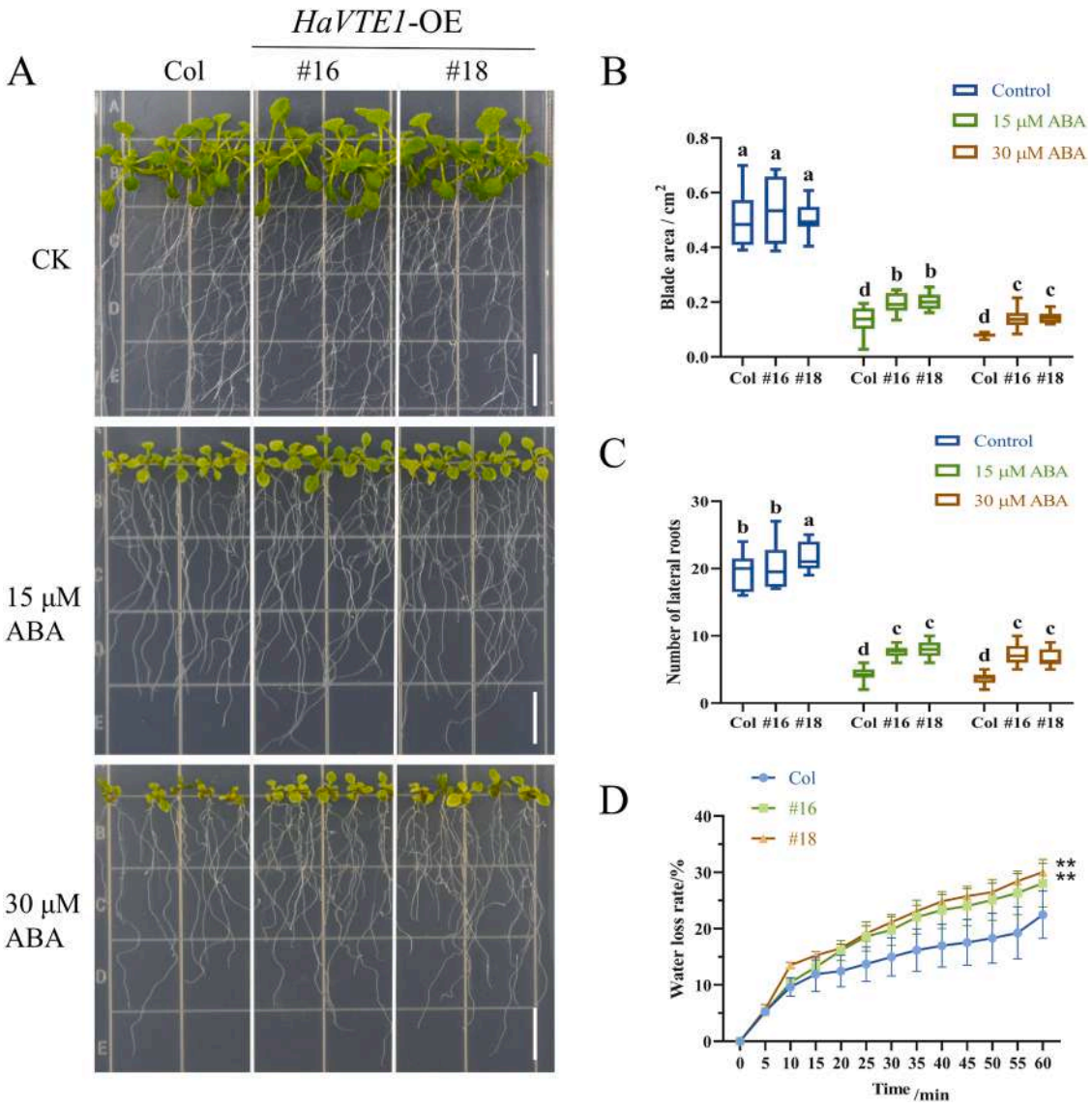

Fig. 5. Overexpression of *HaVTE1* decreases ABA sensitivity in Arabidopsis. (A-C) Photographs (A) and measurements of blade area (B) and amounts of lateral roots (C) of WT and *HaVTE1*-OE lines (#16 and #18) supplemented with ABA. Five-day-old seedlings grown on 0.5 × MS were transferred to new solid agar plates supplemented with 0, 15, or 30 μM ABA. Photographs were taken after 12 d growth on the supplemented media. All values are means (±SE) from three independent experiments (15 seedlings per experiment). a, b, c and d indicate significant differences by two-way ANOVA ($p < 0.01$). **(D)** Water loss rate from detached leaves of WT and *HaVTE1*-OE lines (#16 and #18). The water loss rate of detached leaves from different plants was measured at the indicated time points in triplicate. Three measurements were averaged at each time point. Data are means ±SEs. $^{**}P < 0.01$ by the Student's *t*-test.

ABA signaling.

3.6. *HaVTE1 negatively affected the key genes in ABA signaling pathway*

To gain insight into the mechanisms by which *HaVTE1* enhances ABA insensitivity, we further investigated the molecular functions of *HaVTE1*. RNA-seq was performed in triplicate using 10-day-old sunflowers transiently overexpression *HaVTE1*, under normal and ABA treatment for 10 days. The results of the RNA-seq analysis revealed substantial transcriptional reprogramming upon ABA treatment, where 3156 genes were up-regulated and 1304 genes were down-regulated (Fig. 8A). Correspondingly, in the *HaVTE1* overexpressing sunflowers, the numbers of up-regulated and down-regulated genes after ABA exposure were 4037 and 2537, respectively (Fig. 8B). Among these, 992 up-regulated genes both in EV (CK vs ABA) and *HaVTE1*-OE (CK vs ABA) were identified, whereas 1002 genes were only up-regulated in *HaVTE1*-OE (CK vs ABA) (Fig. 8C). Concerning the down-regulated gene sets, 434 were shared between both the EV (control versus ABA) and *HaVTE1*-OE (control versus ABA) groups, while an additional 986 genes were exclusively down-regulated in the *HaVTE1*-OE (control versus ABA) group (Fig. 8D).

To categorize the functional roles of differentially expressed genes (DEGs) resulting from *HaVTE1* overexpression, we performed Gene Ontology (GO) enrichment analysis on the four gene cohorts identified in the RNA-seq study (Fig. S8). Remarkably, the analysis revealed that many down-regulated genes in response to ABA signaling were associated with abiotic stress pathways (Fig. S8C and D). A focused examination of the ABA receptor gene family, *PYRABACTIN RESISTANCE 1/PYRABACTIN RESISTANCE 1-Like* (*PYR1/PYL*), revealed that these genes exhibited elevated transcript levels in *HaVTE1*-overexpressing plants under normal conditions. The results illustrated that although *PYR1/PYLs* had a higher transcript level in the *HaVTE1*-OE plant than in EV under normal conditions, the expression of *PYR1/PYLs* was markedly suppressed by ABA treatment in both EV and *HaVTE1*-OE, indicating

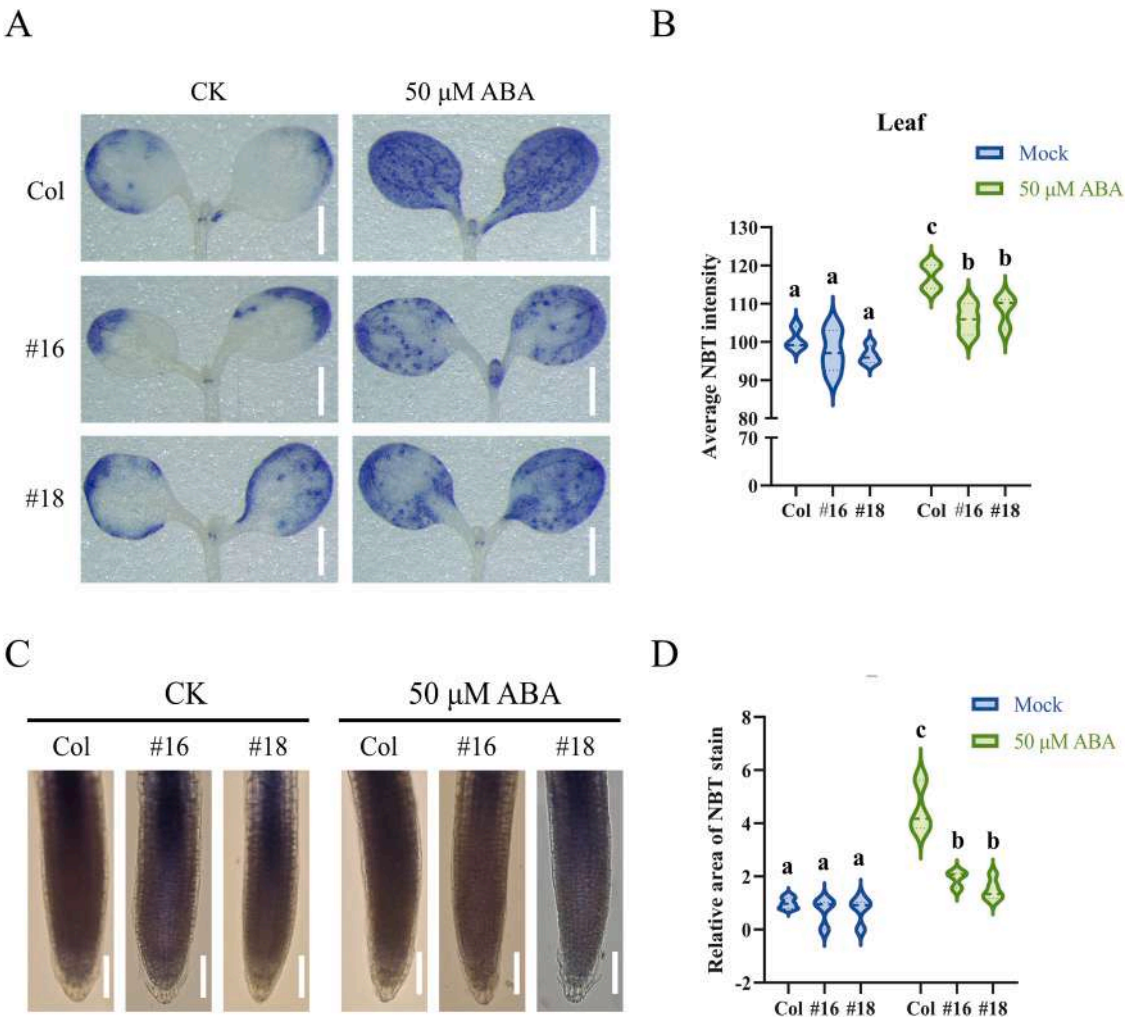

Fig. 6. ***HaVTE1*** **decreases ABA sensitivity by scavenging superoxide contents. (A-B)** Light microscope images of leaves of Col, *HaVTE1*-OE lines (#16 and #18) leaves ($n = 4$) stained with NBT after 50 μM ABA treatment. Bars = 0.5 mm. **(B)** Quantification of NBT staining intensity in Col and *HaVTE1*-OE lines (#16 and #18) leaves after 50 μM ABA treatment for 3 h. Bar graphs show means. Error bars represent ± SE. a, b and c indicate significant differences by two-way ANOVA ($p < 0.01$). **(C-D)** Light microscope images of roots of Col, *HaVTE1*-OE lines (#16 and #18) roots ($n = 4$) stained with NBT after 50 μM ABA treatment. Bars = 0.1 mm. **(D)** Relative area of NBT stain in Col, *HaVTE1*-OE lines (#16 and #18) roots after 50 μM ABA treatment for 3 h. Bar graphs show means. Error bars represent ± SE. a, b and c indicate significant differences by two-way ANOVA ($p < 0.01$).

that *HaVTE1* induced *PYR1/PYLs* expression under normal condition (Fig. 8E). In addition to *PYR1/PYLs*, a systematic survey of genes related to the ABA signaling pathway revealed that the expression of *protein phosphatase 2 C* (*PP2C*), *SNF1-related protein kinases 2* (*SnRK2s*) and *ABI5*-like significantly decreased in *HaVTE1*-OE lines comparing to EV plants (Fig. 8E).These changes were consistent with the insensitive phenotype of *HaVTE1*-OE lines.

To confirm the effect of *HaVTE1* on these ABA pathway-related genes, the promoters of 6 genes (*LOC110884474*, *LOC110880238*, *LOC110912722*, *LOC110885370*, *LOC110894640*, *LOC110889853*) were recombined into pGreen-0800-LUC vector to generate reporter constructs. Then we transformed these reporters with different effectors (empty GFP and HaVTE1) into young tobacco leaves. The promoter of *HaPYL4 (LOC110884474)* was employed as a positive control, whose expression was induced by *HaVTE1* (Fig. 8 E and F). Results revealed that HaVTE1 can significantly inhibit the activity of the *HaPP2C*, *HaSnRK2* and *HaABI5L* promoters, which was consistent to the result of RNA-seq (Fig. 8E and F). In summary, the data suggest that overexpression of *HaVTE1* impedes the ABA signaling cascade and assists in the removal of superoxide radicals (Figs. 6 and 7), thereby contributing to the ABA-insensitive phenotype displayed by the *HaVTE1*-OE plants (Fig. 8G). These findings consolidate our understanding of *HaVTE1*'s role in modulating ABA-mediated stress response pathways.

4. Discussion

In this study, we collected several lines to study the function of *HaVTE1* in response to abiotic stress. Firstly, we conducted a phylogenetic tree of the VTE1 protein across 155 diverse species, revealing that TCs enzymes are highly conserved in evolution. Secondly, our qRT-PCR results showed that *HaVTE1* was ubiquitously expressed in sunflowers and was induced by MeJA and ABA treatments. Thirdly, we constructed transgenic plants of *HaVTE1* in sunflower or Arabidopsis and confirmed that *HaVTE1* participates in the ABA pathway. Finally, our molecular and biochemical experiments revealed that *HaVTE1* blocked the upstream of the ABA signaling cascade, concurrently facilitating the scavenging of superoxide radicals, resulting in reduced sensitivity to ABA of *HaVTE1* overexpression plants. These results deepen our understanding of the molecular mechanisms of ABA signaling and abiotic stress regulation in sunflower.

4.1. *HaVTE1 affects multi-level of ABA signal transduction pathway*

Transcriptome analysis and effector–reporter luciferase assay

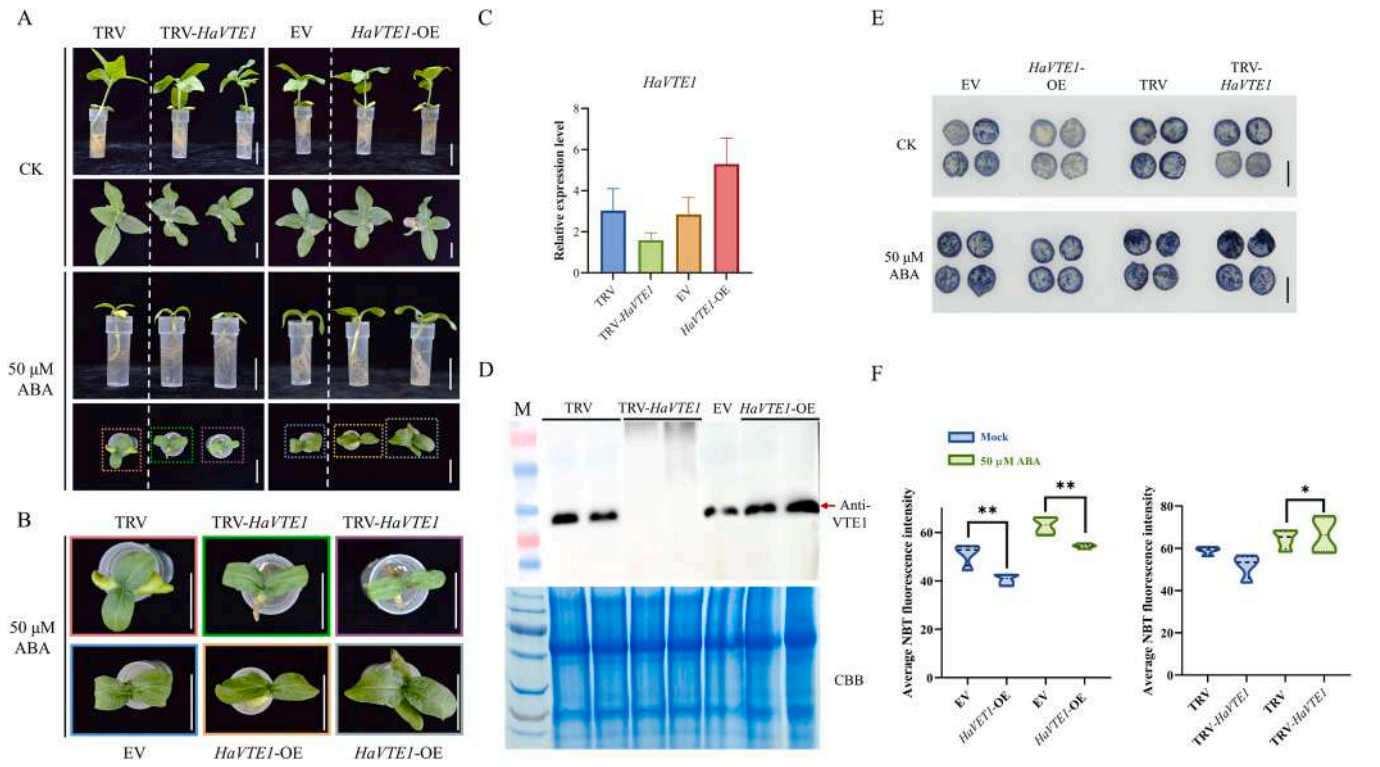

Fig. 7. Overexpression of *HaVTE1* decreases ABA sensitivity in sunflowers. (A-B) Phenotypes of transient transgenic sunflowers under ABA stress for 10 days. All the bars in photographs are equal to 3 cm. EV, empty vector. **(B)** Magnified images from Fig. 7A. Colors represent correspondence. **(C)** Relative expression of *HaVTE1* in empty vector and transient transgenic sunflowers. Data presented are means of three biological replicates (±SE). EV, empty vector. *HaTubulin* was used as a control. **(D)** Expression of HaVTE1 protein in transgenic sunflowers. The total protein was extracted from leave tissues of sunflower and then detected by immunoblot analysis using anti-VTE1. CBB: Coomassie brilliant blue staining. **(E)** Images of leaves of empty vector and transient transgenic sunflowers leaves stained with NBT overnight after 3 h 50 μM ABA treatment. Bars = 0.5 cm. Every leaf was obtained from different individuals ($n = 4$) using a hole puncher. **(F)** Average fluorescence intensity of NBT stain in empty vector and transient transgenic sunflower leaves ($n = 4$) after 50 μM ABA treatment for 6 h. Bar graphs show means. Error bars represent ± SE. $^{**}P < 0.01$ by the Student's *t*-test.

revealed the molecular mechanism of *HaVTE1* in responding to ABA by hindering the ABA signal transduction cascades (Fig. 8). Many proteins regulate ABA signaling in a multi-level manner. Maize WRKY transcription factor ZmWRKY79 positively regulates drought tolerance by elevating NCED3 and AAO3 expression during ABA biosynthesis (Gulzar et al., 2021). The core ABA signal transduction is composed of ABA receptors PYR/PYL/RCARs, PP2C, SnRK2s and the transcriptional factors which can be activated by the phosphorylation function of SnRK2s, such as ABI5 (Danquah et al., 2014). Moreover, ABI5 is a central factor in the GA - ABA antagonism network in seed germination (Li et al., 2022). RGL2, a DELLA protein, can up-regulate the transcript level of *ABI5* (Piskurewicz et al., 2008; Sheerin and Hiltbrunner, 2017). ABI5 directly promotes *PYR/PYL/RCAR* gene expression, strengthening the ABA signal in a positive feedback pattern (Zhao et al., 2020). Combined with the germination phenotype of *HaVTE1* overexpression lines (Fig. S9) and RNA-seq analysis, luciferase assay, we confirmed that *HaVTE1* negatively regulated the transcript level of *ABI5* indirectly. Meanwhile, *HaVTE1* affected *PYR/PYL/RCARs*, *PP2C* and *SnRK2* gene expression to some extent, however, these genes are relatively located upstream of the ABA signal cascade compared with ABI5, which can directly activate ABA-respond genes. Therefore, we concluded that *HaVTE1* mainly regulated the ABA signal pathway through controlling *ABI5* expression.

4.2. *HaVTE1 is transcriptional regulated by environmental stimuli*

By analyzing the *cis*-elements within the *HaVTE1* promoter, we found environmental stimuli response motifs were enriched and confirmed these regulations by mining the transcriptome data including many abiotic stress treatments (Fig. 4A-B). We hypothesized that some stress-related transcription factors like WRKYs, bZIPs and Dofs may regulate the expression of *HaVTE1* in responding to environmental stimuli.

WRKY transcription factor, recognizing W-box in the promoter of target genes, comprehensively participates in plant physiological processes, especially ABA response (Xie et al., 2005). For instance, during seed germination and post-germination growth, AtWRKY40, AtWRKY18 and AtWRKY60 are located in the nucleus, inhibiting the expression of ABA response genes (Shang et al., 2010). AtWRKY40, AtWRKY18 and AtWRKY60 are located upstream of ABA signal transduction, while AtWRKY63 functions downstream. When PYR/PYL/RCAR senses ABA, ABI5 is phosphorylated and activated by SnRK2 kinase, which in turn activates the transcription of AtWRKY63 (Ren et al., 2010). Two W-box (TTGAC motif) are presented in the *HaVTE1* promoter indicating that HaWRKYs may regulate *HaVTE1* expression under ABA signal. Additionally, 3 ABA-responsive elements (ABREs) were also identified within the promoter of *HaVTE1* (Fig. 4A), implying that ABRE binding factor (ABF) / bZIP might regulate the transcript level of *HaVTE1* (Choi et al., 2000). Overexpression of *ABF3* or *ABF4* confers plant ABA hypersensitivity (Kang et al., 2002). Notably, ABI5 belongs to the ABF / bZIP transcription factor. Whether there exists a feedback regulation between HaVTE1 and ABI5 remains unclear. Generally, we supposed that some WRKYs / ABFs can regulate *HaVTE1* expression in response to the ABA signal.

Additionally, the transcriptome sequencing datasets showed that ABA dramatically induced *HaVTE1* expression while GA strongly inhibited *HaVTE1* expression, suggesting that *HaVTE1* possibly participates in the regulation of seed germination (Fig. 4B) (Abley et al., 2021; Ali et al., 2022). Our germination experiment revealed that

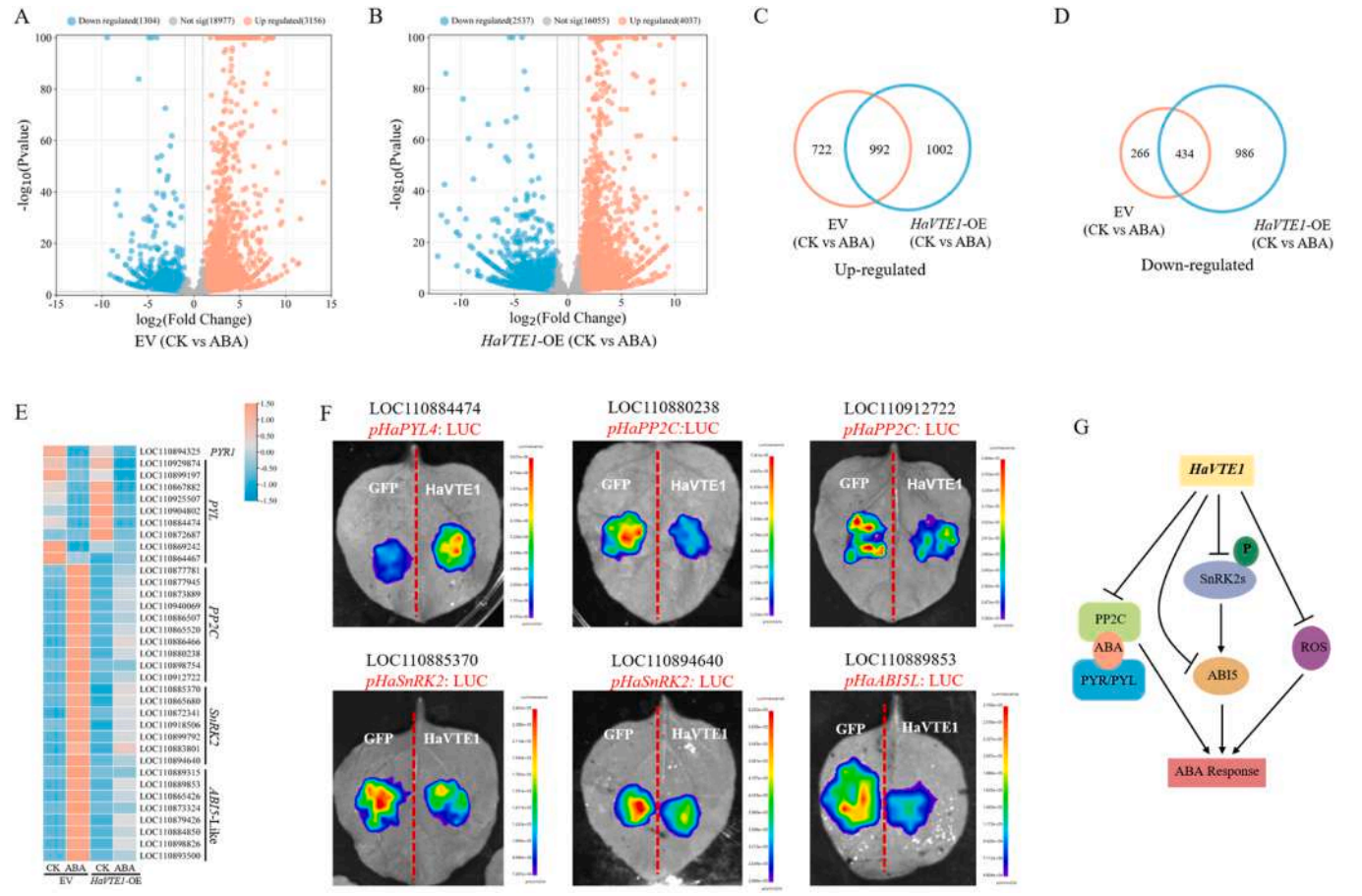

Fig. 8. Genome-wide transcriptome profiling by RNA-seq analysis of EV and *HaVTE1*-OE with or without ABA treatment in sunflowers. (A-B) Volcano plot of significant gene patterns. Log_2(Fold Change) > 1 or < -1 and $p < 0.05$. Red plots represent up-regulated genes, and blue plots represent down-regulated genes. (C-D) Venn diagram of differentially expressed genes (DEGs). (C) up-regulated DEGs, (D) down-regulated DEGs. Red circles represent the DEGs of EV (CK vs ABA), and blue circles represent the DEGs of *HaVTE1*-OE (CK vs ABA). (E) Analysis of ABA signaling pathway-related DEGs. The colour scale indicates Log_2(Fold Change) in mRNA abundance. PYR1, PYRABACTIN RESISTANCE 1; PYL, PYR1-Like; PP2C, protein phosphatase; SnRK2, SNF1-related protein kinase 2; ABI5, ABA insensitivity 5. (F) The luciferase reporter assay of HaVTE1 and ABA-signaling pathway. HaVTE1 suppressed the transcription of the *HaPP2C*, *HaSnRK2* and *HaABI5L* promoters. The promoter of *HaPYL4* was used as a positive control. (G) Proposed model of *HaVTE1* in ABA response pathway. *HaVTE1* decreases ABA sensitivity by negatively regulating the gene expression of *SnRK2s*, *PP2C* and *ABI-5* and scavenging superoxide contents in sunflower.

over-expression of *HaVTE1* can promote seed germination, which conformed to the assumption and further confirmed that *HaVTE1* could decrease plants' ABA sensitivity (Fig. S9A-B). Meanwhile, there are several Dof transcription factor specific binding sites (T/AAAAG) in the *HaVTE1* promoter. Dof protein family is known for its role in seed germination. For example, AtDof3.7 directly suppresses the expression of GA biosynthetic and catabolic genes, *GA3ox1* and *CYP707A2*, resulting in disturbed GA/ABA ratio level and affecting seed germination (Boccaccini et al., 2016; Gabriele et al., 2010; Papi et al., 2000). Generally, it is possible that Dof family proteins may regulate *HaVTE1* expression and result in the early germination phenotype of *HaVTE1*-OE (Fig.S9).

4.3. the role of HaVTE1 in ABA-JA crosstalk

We showed that *HaVTE1* overexpression lines had reduced sensitivity phenotypes to ABA and MeJA, demonstrating that HaVTE1 acts as a negative regulator in ABA and JA signaling. These results suggested the role of *HaVTE1* in the ABA-MeJA crosstalk. Notably, several ABA signaling core factors have been reported to function in integrating ABA and JA signals. PYL6, with ABA present, strongly binds to MYC2, a master protein in the JA signal pathway, modifying its transcriptional activity, and promoting the expression of *JAZ8* (Aleman et al., 2016). The transcription factors ARF10 and ARF16 positively participate in the ABA-JA synergistic effect, and overexpressing ARF16 partially recovers the hypersensitive phenotype of the plants that overaccumulate JAZ but cannot sense JA signaling under ABA and JA treatment. Moreover, ARF10, ARF16 and ABI5 can form a complex in physics and the function of ARF16 to activate JA-ABA response is required for ABI5 (Mei et al., 2023). Collectively, we speculated that *HaVTE1* might integrate the ABA-JA signal by fine-tuning *PYR/PYL/RCARs* and *ABI5* expression.

4.4. HaVTE1 participates in the process of leaf development

Notably, we found that the number of rosette leaves and bolting in *HaVTE1*-OE lines was remarkably higher than in WT. Conversely, the single-leaf area and the diameter of the rosette leaf of *HaVTE1*-OE lines were less than WT. Meanwhile, the leaf shape was changed, embodied in the lower ratio of leaf length to leaf width. Besides, overexpressing *HaVTE1* increased the number of bolting (Fig. S6). Based on these phenotypes, we supposed that *HaVTE1* may participate in the strigolactone-related pathway. Strigolactones (SLs) are carotenoid-derived phytohormones that control plant development, including shoot branching and leaf morphology (Wang et al., 2015; Waters et al., 2017). The leaf number and shape phenotypes of *HaVTE1*-OE lines are similar to those *max3–9* mutant and opposite to *smxl6/7/8* mutant in Arabidopsis. MAX3 is a vital enzyme in SLs synthesis and SMXL6/7/8 protein is the repressor of SLs signal, which suggests that the SLs content

might be lower or / and the SL signal be interfered in *HaVTE1*-OE line, meaning that *HaVTE1* is a negative factor in SLs pathway (Wang et al., 2015). Taken together, *HaVTE1* confers plant insensitivity to several phytohormones (ABA, MeJA and SLs).

In summary, we have uncovered the evolutionary process of VTE1 and revealed a mechanism of how *HaVTE1* works during a plant faces abiotic stress, which lays a foundation for the further study of the molecular regulation mechanism of *HaVTE1* and is exploited to improve stress tolerance in crop plants.

5. Conclusion

In this study, we revealed the highly conserved evolutionary trace of VTE1. The expression profiling of *HaVTE1* depicted that the *HaVTE1* expression migrated from foliar tissues to both floret and root tissues during the vegetative to reproductive phase transition and was induced by MeJA and ABA treatments. We further explored that *HaVTE1* blocked the upstream of the ABA signaling cascade, concurrently facilitating the scavenging of superoxide radicals, resulting in reduced sensitivity to ABA of *HaVTE1* overexpression plants.

Funding

This research received the Starting Research Fund from Hangzhou Normal University (2019QDL015).

CRediT authorship contribution statement

Zhonghua Lei: Resources. **Juncheng Zhang:** Formal analysis. **Hada Wuriyanghan:** Methodology. **Yingwei Wang:** Writing – original draft, Formal analysis, Data curation, Conceptualization. **Qixiu Huang:** Resources. **Lijun Xiang:** Resources. **Chenchang Wang:** Data curation. **Xinxin Li:** Data curation. **Maohong Cai:** Writing – review & editing, Project administration. **Jiafeng Gu:** Writing – original draft, Data curation. **Tao Chen:** Writing – review & editing, Supervision, Funding acquisition. **Qinzong Zeng:** Validation, Methodology. **Qinyu Xie:** Data curation. **Yuliang Han:** Data curation.

Declaration of Competing Interest

The authors declare that they have no known competing financial interests or personal relationships that could have appeared to influence the work reported in this paper.

Appendix A. Supporting information

Supplementary data associated with this article can be found in the online version at doi:10.1016/j.indcrop.2024.119850.

Data Availability

Data will be made available on request.

References

Abley, K., Formosa-Jordan, P., Tavares, H., Chan, E.Y., Afsharinafar, M., Leyser, O., Locke, J.C., 2021. An ABA-GA bistable switch can account for natural variation in the variability of Arabidopsis seed germination time. Elife *10*. https://doi.org/10.7554/eLife.59485.

Aleman, F., Yazaki, J., Lee, M., Takahashi, Y., Kim, A.Y., Li, Z., Kinoshita, T., Ecker, J.R., Schroeder, J.I., 2016. An ABA-increased interaction of the PYL6 ABA receptor with MYC2 transcription factor: a putative link of ABA and JA signaling. Sci. Rep. *6*, 28941. https://doi.org/10.1038/srep28941.

Ali, F., Qanmber, G., Li, F., Wang, Z., 2022. Updated role of ABA in seed maturation, dormancy, and germination. J. Adv. Res *35*, 199–214. https://doi.org/10.1016/j.jare.2021.03.011.

Badouin, H., Gouzy, J., Grassa, C.J., Murat, F., Staton, S.E., Cottret, L., Lelandais-Brière, C., Owens, G.L., Carrère, S., Mayjonade, B., Legrand, L., Gill, N., Kane, N.C., Bowers, J.E., Hubner, S., Bellec, A., Bérard, A., Bergès, H., Blanchet, N., Langlade, N. B., 2017. The sunflower genome provides insights into oil metabolism, flowering and Asterid evolution. Nature *546* (7656), 148–152. https://doi.org/10.1038/nature22380.

Bailey, T.L., Johnson, J., Grant, C.E., Noble, W.S., 2015. The MEME suite. Nucleic Acids Res. *43* (W1), W39–W49. https://doi.org/10.1093/nar/gkv416.

Boccaccini, A., Lorrai, R., Ruta, V., Frey, A., Mercey-Boutet, S., Marion-Poll, A., Tarkowská, D., Strnad, M., Costantino, P., Vittorioso, P., 2016. The DAG1 transcription factor negatively regulates the seed-to-seedling transition in Arabidopsis acting on ABA and GA levels. BMC Plant Biol. *16* (1), 198. https://doi.org/10.1186/s12870-016-0890-5.

Burley, S.K., Bhikadiya, C., Bi, C., Bittrich, S., Chao, H., Chen, L., Craig, P.A., Crichlow, G. V., Dalenberg, K., Duarte, J.M., Dutta, S., Fayazi, M., Feng, Z., Flatt, J.W., Ganesan, S., Ghosh, S., Goodsell, D.S., Green, R.K., Guranovic, V., Zardecki, C., 2022. RCSB Protein Data Bank (RCSB.org): delivery of experimentally-determined PDB structures alongside one million computed structure models of proteins from artificial intelligence/machine learning. Nucleic Acids Res. *51* (D1), D488–D508. https://doi.org/10.1093/nar/gkac1077.

Cabello, J.V., Giacomelli, J.I., Gómez, M.C., Chan, R.L., 2017. The sunflower transcription factor HaHB11 confers tolerance to water deficit and salinity to transgenic Arabidopsis and alfalfa plants. J. Biotechnol. *257*, 35–46. https://doi.org/10.1016/j.jbiotec.2016.11.017.

Cabello, J.V., Giacomelli, J.I., Piattoni, C.V., Iglesias, A.A., Chan, R.L., 2016. The sunflower transcription factor HaHB11 improves yield, biomass and tolerance to flooding in transgenic Arabidopsis plants. J. Biotechnol. *222*, 73–83. https://doi.org/10.1016/j.jbiotec.2016.02.015.

Cela, J., Tweed, J.K.S., Sivakumaran, A., Lee, M.R.F., Mur, L.A.J., Munné-Bosch, S., 2018. An altered tocopherol composition in chloroplasts reduces plant resistance to Botrytis cinerea. Plant Physiol. Biochem. *127*, 200–210. https://doi.org/10.1016/j.plaphy.2018.03.033.

Ceylan, Y., Altunoglu, Y.C., Horuz, E., 2023. HSF and Hsp Gene Families in sunflower: a comprehensive genome-wide determination survey and expression patterns under abiotic stress conditions. Protoplasma *260* (6), 1473–1491. https://doi.org/10.1007/s00709-023-01862-6.

Chen, C., Chen, H., Zhang, Y., Thomas, H.R., Frank, M.H., He, Y., Xia, R., 2020. TBtools: an integrative toolkit developed for interactive analyses of big biological Data. Mol. Plant *13* (8), 1194–1202. https://doi.org/10.1016/j.molp.2020.06.009.

Choi, H.-i, Hong, J.-h, Ha, J.-o, Kang, J.-y, Kim, S.Y., 2000. ABFs, a family of ABA-responsive element binding factors. J. Biol. Chem. *275* (3), 1723–1730. https://doi.org/10.1074/jbc.275.3.1723.

Danquah, A., de Zelicourt, A., Colcombet, J., Hirt, H., 2014. The role of ABA and MAPK signaling pathways in plant abiotic stress responses. Biotechnol. Adv. *32* (1), 40–52. https://doi.org/10.1016/j.biotechadv.2013.09.006.

Dezar, C.A., Gago, G.M., González, D.H., Chan, R.L., 2005. Hahb-4, a sunflower homeobox-leucine zipper gene, is a developmental regulator and confers drought tolerance to Arabidopsis thaliana plants. Transgenic Res. *14* (4), 429–440. https://doi.org/10.1007/s11248-005-5076-0.

Ellouzi, H., Hamed, K.B., Cela, J., Müller, M., Abdelly, C., Munné-Bosch, S., 2013. Increased sensitivity to salt stress in tocopherol-deficient Arabidopsis mutants growing in a hydroponic system. Plant Signal Behav. *8* (2), e23136. https://doi.org/10.4161/psb.23136.

Gabriele, S., Rizza, A., Martone, J., Circelli, P., Costantino, P., Vittorioso, P., 2010. The Dof protein DAG1 mediates PIL5 activity on seed germination by negatively regulating GA biosynthetic gene AtGA3ox1. Plant J. *61* (2), 312–323. https://doi.org/10.1111/j.1365-313X.2009.04055.x.

Gulzar, F., Fu, J., Zhu, C., Yan, J., Li, X., Meraj, T.A., Shen, Q., Hassan, B., Wang, Q., 2021. Maize WRKY transcription factor ZmWRKY79 positively regulates drought tolerance through elevating ABA biosynthesis. Int J. Mol. Sci. *22* (18). https://doi.org/10.3390/ijms221810080.

Han, Y., Cai, M., Zhang, S., Chai, J., Sun, M., Wang, Y., Xie, Q., Chen, Y., Wang, H., Chen, T., 2022. Genome-wide identification of AP2/ERF transcription factor family and functional analysis of DcAP2/ERF#96 associated with abiotic stress in dendrobium catenatum. Int J. Mol. Sci. *23* (21). https://doi.org/10.3390/ijms232113603.

Havaux, M., Eymery, F., Porfirova, S., Rey, P., Dörmann, P., 2005. Vitamin E protects against photoinhibition and photooxidative stress in Arabidopsis thaliana. Plant Cell *17* (12), 3451–3469. https://doi.org/10.1105/tpc.105.037036.

Hewage, K.A.H., Yang, J.F., Wang, D., Hao, G.F., Yang, G.F., Zhu, J.K., 2020. Chemical manipulation of abscisic acid signaling: a new approach to abiotic and biotic stress management in agriculture. Adv. Sci. (Weinh.) *7* (18), 2001265. https://doi.org/10.1002/advs.202001265.

Hofius, D., Hajirezaei, M.R., Geiger, M., Tschiersch, H., Melzer, M., Sonnewald, U., 2004. RNAi-mediated tocopherol deficiency impairs photoassimilate export in transgenic potato plants. Plant Physiol. *135* (3), 1256–1268. https://doi.org/10.1104/pp.104.043927.

Jiang, Z., Zhao, Q., Bai, R., Yu, R., Diao, P., Yan, T., Duan, H., Ma, X., Zhou, Z., Fan, Y., Wuriyanghan, H., 2021. Host sunflower-induced silencing of parasitism-related genes confers resistance to invading Orobanche cumana. Plant Physiol. *185* (2), 424–440. https://doi.org/10.1093/plphys/kiaa018.

Kang, J.Y., Choi, H.I., Im, M.Y., Kim, S.Y., 2002. Arabidopsis basic leucine zipper proteins that mediate stress-responsive abscisic acid signaling. Plant Cell *14* (2), 343–357. https://doi.org/10.1105/tpc.010362.

Kanwischer, M., Porfirova, S., Bergmüller, E., Dörmann, P., 2005. Alterations in tocopherol cyclase activity in transgenic and mutant plants of arabidopsis affect tocopherol content, tocopherol composition, and oxidative stress. Plant Physiol. *137* (2), 713–723. https://doi.org/10.1104/pp.104.054908.

Kim, S.E., Bian, X., Lee, C.J., Park, S.U., Lim, Y.H., Kim, B.H., Park, W.S., Ahn, M.J., Ji, C. Y., Yu, Y., Xie, Y., Kwak, S.S., Kim, H.S., 2021. Overexpression of 4-hydroxyphenylpyruvate dioxygenase (IbHPPD) increases abiotic stress tolerance in transgenic sweetpotato plants. Plant Physiol. Biochem *167*, 420–429. https://doi.org/10.1016/j.plaphy.2021.08.025.

Kobayashi, N., DellaPenna, D., 2008. Tocopherol metabolism, oxidation and recycling under high light stress in Arabidopsis. Plant J. *55* (4), 607–618. https://doi.org/10.1111/j.1365-313X.2008.03539.x.

Ksas, B., Légeret, B., Ferretti, U., Chevalier, A., Pospíšil, P., Alric, J., Havaux, M., 2018. The plastoquinone pool outside the thylakoid membrane serves in plant photoprotection as a reservoir of singlet oxygen scavengers. Plant Cell Environ. *41* (10), 2277–2287. https://doi.org/10.1111/pce.13202.

Kumar, A., Prasad, A., Sedlářová, M., Ksas, B., Havaux, M., Pospíšil, P., 2020. Interplay between antioxidants in response to photooxidative stress in Arabidopsis. Free Radic. Biol. Med *160*, 894–907. https://doi.org/10.1016/j.freeradbiomed.2020.08.027.

Kumar, S., Stecher, G., Tamura, K., 2016. MEGA7: molecular evolutionary genetics analysis version 7.0 for bigger datasets. Mol. Biol. Evol. *33* (7), 1870–1874. https://doi.org/10.1093/molbev/msw054.

Lee, K., Lee, S.M., Park, S.R., Jung, J., Moon, J.K., Cheong, J.J., Kim, M., 2007.). Overexpression of Arabidopsis homogentisate phytyltransferase or tocopherol cyclase elevates vitamin E content by increasing gamma-tocopherol level in lettuce (Lactuca sativa L.). Mol. Cells *24* (2), 301–306.

Lescot, M., Déhais, P., Thijs, G., Marchal, K., Moreau, Y., Van de Peer, Y., Rouzé, P., Rombauts, S., 2002. PlantCARE, a database of plant cis-acting regulatory elements and a portal to tools for in silico analysis of promoter sequences. Nucleic Acids Res. *30* (1), 325–327. https://doi.org/10.1093/nar/30.1.325.

Li, Z., Luo, X., Wang, L., Shu, K., 2022. ABSCISIC ACID INSENSITIVE 5 mediates light-ABA/gibberellin crosstalk networks during seed germination. J. Exp. Bot. *73* (14), 4674–4682. https://doi.org/10.1093/jxb/erac200.

Liu, X., Hua, X., Guo, J., Qi, D., Wang, L., Liu, Z., Jin, Z., Chen, S., Liu, G., 2008. Enhanced tolerance to drought stress in transgenic tobacco plants overexpressing VTE1 for increased tocopherol production from Arabidopsis thaliana. Biotechnol. Lett. *30* (7), 1275–1280. https://doi.org/10.1007/s10529-008-9672-y.

Lu, S., Wang, J., Chitsaz, F., Derbyshire, M.K., Geer, R.C., Gonzales, N.R., Gwadz, M., Hurwitz, D.I., Marchler, G.H., Song, J.S., Thanki, N., Yamashita, R.A., Yang, M., Zhang, D., Zheng, C., Lanczycki, C.J., Marchler-Bauer, A., 2020. CDD/SPARCLE: the conserved domain database in 2020. d268 Nucleic Acids Res *48* (D1), D265. https://doi.org/10.1093/nar/gkz991.

Ma, J., Qiu, D., Pang, Y., Gao, H., Wang, X., Qin, Y., 2020. Diverse roles of tocopherols in response to abiotic and biotic stresses and strategies for genetic biofortification in plants. Mol. Breed. *40* (2), 18. https://doi.org/10.1007/s11032-019-1097-x.

Manavella, P.A., Arce, A.L., Dezar, C.A., Bitton, F., Renou, J.P., Crespi, M., Chan, R.L., 2006. Cross-talk between ethylene and drought signalling pathways is mediated by the sunflower Hahb-4 transcription factor. Plant J. *48* (1), 125–137. https://doi.org/10.1111/j.1365-313X.2006.02865.x.

Mei, S., Zhang, M., Ye, J., Du, J., Jiang, Y., Hu, Y., 2023. Auxin contributes to jasmonate-mediated regulation of abscisic acid signaling during seed germination in Arabidopsis. Plant Cell *35* (3), 1110–1133. https://doi.org/10.1093/plcell/koac362.

Moschen, S., Di Rienzo, J.A., Higgins, J., Tohge, T., Watanabe, M., González, S., Rivarola, M., García-García, F., Dopazo, J., Hopp, H.E., Hoefgen, R., Fernie, A.R., Paniego, N., Fernández, P., Heinz, R.A., 2017. Integration of transcriptomic and metabolic data reveals hub transcription factors involved in drought stress response in sunflower (Helianthus annuus L.). Plant Mol. Biol. *94* (4-5), 549–564. https://doi.org/10.1007/s11103-017-0625-5.

Nakashima, K., Yamaguchi-Shinozaki, K., 2013. ABA signaling in stress-response and seed development. Plant Cell Rep. *32* (7), 959–970. https://doi.org/10.1007/s00299-013-1418-1.

Ouyang, S., He, S., Liu, P., Zhang, W., Zhang, J., Chen, S., 2011. The role of tocopherol cyclase in salt stress tolerance of rice (Oryza sativa). Sci. China Life Sci. *54* (2), 181–188. https://doi.org/10.1007/s11427-011-4138-1.

Papi, M., Sabatini, S., Bouchez, D., Camilleri, C., Costantino, P., Vittorioso, P., 2000. Identification and disruption of an Arabidopsis zinc finger gene controlling seed germination. Genes Dev. *14* (1), 28–33.

Piskurewicz, U., Jikumaru, Y., Kinoshita, N., Nambara, E., Kamiya, Y., Lopez-Molina, L., 2008. The gibberellic acid signaling repressor RGL2 inhibits Arabidopsis seed germination by stimulating abscisic acid synthesis and ABI5 activity. Plant Cell *20* (10), 2729–2745. https://doi.org/10.1105/tpc.108.061515.

Provencher, L.M., Miao, L., Sinha, N., Lucas, W.J., 2001. Sucrose export defective1 encodes a novel protein implicated in chloroplast-to-nucleus signaling. Plant Cell *13* (5), 1127–1141. https://doi.org/10.1105/tpc.13.5.1127.

Raineri, J., Ribichich, K.F., Chan, R.L., 2015. The sunflower transcription factor HaWRKY76 confers drought and flood tolerance to Arabidopsis thaliana plants without yield penalty. Plant Cell Rep. *34* (12), 2065–2080. https://doi.org/10.1007/s00299-015-1852-3.

Ramu, V.S., Paramanantham, A., Ramegowda, V., Mohan-Raju, B., Udayakumar, M., Senthil-Kumar, M., 2016. Transcriptome analysis of sunflower genotypes with contrasting oxidative stress tolerance reveals individual- and combined- biotic and abiotic stress tolerance mechanisms. PLoS One *11* (6), e0157522. https://doi.org/10.1371/journal.pone.0157522.

Rastogi, A., Yadav, D.K., Szymańska, R., Kruk, J., Sedlářová, M., Pospíšil, P., 2014. Singlet oxygen scavenging activity of tocopherol and plastochromanol in Arabidopsis thaliana: relevance to photooxidative stress. Plant Cell Environ. *37* (2), 392–401. https://doi.org/10.1111/pce.12161.

Ren, X., Chen, Z., Liu, Y., Zhang, H., Zhang, M., Liu, Q., Hong, X., Zhu, J.K., Gong, Z., 2010. ABO3, a WRKY transcription factor, mediates plant responses to abscisic acid and drought tolerance in Arabidopsis. Plant J. *63* (3), 417–429. https://doi.org/10.1111/j.1365-313X.2010.04248.x.

Sattler, S.E., Gilliland, L.U., Magallanes-Lundback, M., Pollard, M., DellaPenna, D., 2004. Vitamin E is essential for seed longevity and for preventing lipid peroxidation during germination. Plant Cell *16* (6), 1419–1432. https://doi.org/10.1105/tpc.021360.

Schneider, C.A., Rasband, W.S., Eliceiri, K.W., 2012. NIH Image to ImageJ: 25 years of image analysis. Nat. Methods *9* (7), 671–675. https://doi.org/10.1038/nmeth.2089.

Shang, Y., Yan, L., Liu, Z.Q., Cao, Z., Mei, C., Xin, Q., Wu, F.Q., Wang, X.F., Du, S.Y., Jiang, T., Zhang, X.F., Zhao, R., Sun, H.L., Liu, R., Yu, Y.T., Zhang, D.P., 2010. The Mg-chelatase H subunit of Arabidopsis antagonizes a group of WRKY transcription repressors to relieve ABA-responsive genes of inhibition. Plant Cell *22* (6), 1909–1935. https://doi.org/10.1105/tpc.110.073874.

Sheerin, D.J., Hiltbrunner, A., 2017. Molecular mechanisms and ecological function of far-red light signalling. Plant, Cell Environ. *40* (11), 2509–2529. https://doi.org/10.1111/pce.12915.

Simancas, B., Munné-Bosch, S., 2015. Interplay between vitamin E and phosphorus availability in the control of longevity in Arabidopsis thaliana. Ann. Bot. *116* (4), 511–518. https://doi.org/10.1093/aob/mcv033.

Song, H., Fu, X., Li, J., Niu, T., Shen, J., Wang, X., Li, Y., Hou, Q., Liu, A., 2022. Phylogenetic analysis and expression profiles of jasmonate ZIM-domain gene family provide insight into abiotic stress resistance in sunflower. Front Plant Sci. *13*, 1010404. https://doi.org/10.3389/fpls.2022.1010404.

Spicher, L., Kessler, F., 2015. Unexpected roles of plastoglobules (plastid lipid droplets) in vitamin K1 and E metabolism. Curr. Opin. Plant Biol. *25*, 123–129. https://doi.org/10.1016/j.pbi.2015.05.005.

Torti, P., Raineri, J., Mencia, R., Campi, M., Gonzalez, D.H., Welchen, E., 2020. The sunflower TLDc-containing protein HaOXR2 confers tolerance to oxidative stress and waterlogging when expressed in maize plants. Plant Sci. *300*, 110626. https://doi.org/10.1016/j.plantsci.2020.110626.

Wang, L., Wang, B., Jiang, L., Liu, X., Li, X., Lu, Z., Meng, X., Wang, Y., Smith, S.M., Li, J., 2015. Strigolactone signaling in arabidopsis regulates shoot development by targeting D53-like SMXL repressor proteins for ubiquitination and degradation. Plant Cell *27* (11), 3128–3142. https://doi.org/10.1105/tpc.15.00605.

Waterhouse, A., Bertoni, M., Bienert, S., Studer, G., Tauriello, G., Gumienny, R., Heer, F. T., de Beer, T.A.P., Rempfer, C., Bordoli, L., Lepore, R., Schwede, T., 2018. SWISS-MODEL: homology modelling of protein structures and complexes. w303 Nucleic Acids Res *46* (W1), W296. https://doi.org/10.1093/nar/gky427.

Waters, M.T., Gutjahr, C., Bennett, T., Nelson, D.C., 2017. Strigolactone signaling and evolution. Annu Rev. Plant Biol. *68*, 291–322. https://doi.org/10.1146/annurev-arplant-042916-040925.

Xie, Z., Zhang, Z.L., Zou, X., Huang, J., Ruas, P., Thompson, D., Shen, Q.J., 2005. Annotations and functional analyses of the rice WRKY gene superfamily reveal positive and negative regulators of abscisic acid signaling in aleurone cells. Plant Physiol. *137* (1), 176–189. https://doi.org/10.1104/pp.104.054312.

Yao, Y., You, J., Ou, Y., Ma, J., Wu, X., Xu, G., 2015. Ultraviolet-B protection of ascorbate and tocopherol in plants related with their function on the stability on carotenoid and phenylpropanoid compounds. Plant Physiol. Biochem. *90*, 23–31. https://doi.org/10.1016/j.plaphy.2015.02.021.

Zhao, H., Nie, K., Zhou, H., Yan, X., Zhan, Q., Zheng, Y., Song, C.P., 2020. ABI5 modulates seed germination via feedback regulation of the expression of the PYR/PYL/RCAR ABA receptor genes. N. Phytol. *228* (2), 596–608. https://doi.org/10.1111/nph.16713.